https://doi.org/10.5194/acp-2022-182
Preprint. Discussion started: 7 April 2022

Atmospheric Chemistry and Physics
Discussions

Effects of Reanalysis Forcing Fields on Ozone Trends from a Chemical Transport Model

Yajuan Li[1], Sandip S. Dhomse[2,3], Martyn P. Chipperfield[2,3], Wuhu Feng[2,4], Andreas Chrysanthou[2], Yuan Xia[1] and Dong Guo[5]

[1]School of Electronic Engineering, Nanjing Xiaozhuang University, Nanjing, China
[2]School of Earth and Environment, University of Leeds, Leeds, UK
[3]National Centre for Earth Observation, University of Leeds, Leeds, UK
[4]National Centre for Atmospheric Science, University of Leeds, Leeds, UK
[5]Key Laboratory of Meteorological Disaster, Ministry of Education/Joint International Research Laboratory of Climate and Environment Change/Collaborative Innovation Center on Forecast and Evaluation of Meteorological Disasters, Nanjing University of Information Science & Technology, Nanjing, China

Correspondence to: Martyn P. Chipperfield (M.Chipperfield@leeds.ac.uk)

Abstract. We use the TOMCAT 3-dimensional (3D) off-line chemical transport model (CTM) forced by two different meteorological reanalysis datasets (ERA-Interim and ERA5) from the European Centre for Medium-Range weather Forecasts (ECMWF) to study stratospheric ozone trends and variability. The model-simulated ozone variations are evaluated against two observation-based data sets. For total column ozone (TCO) we use the Copernicus Climate Change Service (C3S) data (1979-2019), while for ozone profiles we use the Stratospheric Water and OzOne Satellite Homogenized (SWOOSH) database (1984-2019). We find that the CTM simulations forced by ERA-Interim (A_ERAI) and ERA5 (B_ERA5) can both successfully reproduce spatial and temporal variations in stratospheric ozone. Modelled TCO anomalies from B_ ERA5 show better agreement with C3S than A_ERAI, especially in northern hemisphere (NH) mid-latitudes, except that it produces large positive biases (> 15 DU) during winter-spring seasons. Ozone profile comparisons against SWOOSH data show larger differences between the two simulations. In the lower stratosphere, which controls the TCO, these are primarily due to differences in transport, whereas in the upper stratosphere they can be directly attributed to the differences in temperatures between the two reanalysis data sets. Although TCO anomalies from B_ERA5 show better agreement with C3S compared to A_ERAI, comparison with SWOOSH data does not confirm that B_ERA5 performs better in simulating the stratospheric ozone profiles. We employ a multi-variate regression model with piecewise linear trends (PWLT) to quantify ozone trends before and after peak stratospheric halogen loading in 1997. This model shows that compared to C3S, TCO recovery trends (since 1998) in simulation B_ERA5 are significantly overestimated in the southern hemisphere (SH) mid-latitudes, while for A_ERAI in the NH mid-latitudes simulated ozone trends remain negative. Similarly, in the lower stratosphere B_ERA5 shows positive ozone recovery trends for both NH and SH mid-latitudes. In contrast, both SWOOSH and A_ERAI show opposite (negative) trends in the NH mid-latitudes. We analyse Age-of-Air (AoA) trends to diagnose transport differences between the two reanalysis data sets. Simulation B_ERA5 shows a positive AoA trend after 1998 and somewhat older age in the NH lower stratosphere compared to A_ERAI, indicating a slower Brewer-Dobson circulation

https://doi.org/10.5194/acp-2022-182
Preprint. Discussion started: 7 April 2022

does not translate into reduced wintertime ozone build-up in the NH extratropical lower stratosphere. Overall, our results show that models forced by the most recent ERA5 reanalyses may not yet be capable of reproducing observed changes in stratospheric ozone, particularly in the lower stratosphere.

1 Introduction

The stratospheric ozone layer protects life on earth from the damaging effects of ultraviolet radiation. The 1987 Montreal Protocol and its subsequent amendments and adjustments have successfully controlled the major anthropogenic ozone-depleting substances (ODSs) leading to a decrease in stratospheric chlorine and bromine and the onset of recovery of the ozone layer (e.g. WMO, 2018). The characteristic details of ozone depletion and the ongoing recovery in recent decades has been investigated using both observations and models (e.g. Solomon et al., 2016; Chipperfield et al., 2017; Dhomse et al., 2018; WMO, 2018 and references therein).

Previous studies consistently report a robust sign of recovery in upper stratospheric ozone after the peak halogen (chlorine and bromine) loading around the year 1997 (e.g. Chipperfield et al., 2017; Weber et al., 2018). Besides the decrease in ODSs, cooling induced by increased greenhouse gases (GHGs) slows the rate of ozone loss, ultimately contributing to the increase in upper stratospheric ozone (e.g. Bekki et al., 2013; Marsh et al., 2016). However, the recovery of ozone in the upper stratosphere does not imply the recovery of the stratospheric or whole atmosphere column ozone. In the lower stratosphere, a region characterised by large interannual variability, the evolution of ozone is much more complicated as its abundance is largely controlled by complex interactions between various chemical and dynamical processes (e.g. WMO, 2014). Even with those complications, it was expected that first signs of ozone recovery (i.e. almost negligible negative ozone trends) would be detectable within a couple of decades after the peak in stratospheric chlorine loading. However, recent observation-based studies show evidence of a continued decline in lower stratospheric ozone since 1998 (e.g. Steinbrecht et al., 2017; Ball et al., 2018, 2019).

Using model simulations, dynamical variability has been proposed as the possible driver that dominates the recent ozone changes in the mid-latitude lower stratosphere (e.g. Chipperfield et al., 2018; Stone et al., 2018). However, inconsistencies have been noted between the observed and model-simulated ozone variations. Ball et al. (2018) reported a significant decrease in lower stratospheric ozone between 60°S and 60°N over the period 1998-2016 using multiple satellite datasets. Furthermore, there was no significant change in total column ozone due to cancellation of opposing trends from increasing tropospheric ozone. They also compared stratospheric partial column ozone trends with two chemistry–climate models (CCMs) run in a “specified-dynamics” configuration constrained with reanalyses, neither of which reproduced the observed lower stratospheric decline, possibly related to limitations in capturing the residual circulation adequately (e.g. Chrysanthou et al., 2019; Orbe et al., 2020a). Subsequently, the negative trends in the mid-latitude lower stratospheric ozone have been identified from reanalysis results and updated satellite datasets (e.g. Wargan et al., 2018; Ball et al., 2019). Chipperfield et al. (2018) demonstrated the ability of TOMCAT/SLIMCAT chemical transport model (CTM) simulations to largely reproduce

https://doi.org/10.5194/acp-2022-182
Preprint. Discussion started: 7 April 2022

Atmospheric Chemistry and Physics Discussions

the observed ozone changes and suggested that atmospheric dynamics plays an important role in controlling ozone in the extra-polar lower stratosphere. They also showed that the effects of trends in short-lived chlorine and bromine compounds on the recent ozone changes are relatively small. Ball et al. (2019) extended their analysis through 2018 and proposed that the global lower stratospheric ozone decrease is continuing despite the large, short-term ozone increase in 2017, which might have been overestimated in CTM simulations by Chipperfield et al. (2018).

Orbe et al. (2020b) showed that a free-running CCM can simulate the ozone decrease in the northern hemisphere lower stratosphere, but the magnitude of ozone changes is significantly weaker than observed, and consistent with weaker residual circulation changes. Ball et al. (2020) also showed that CCMVal models run with a future ODS and GHG scenario (REF-C2) exhibit a decline in tropical lower stratospheric ozone similar to that observed, but most CCMs do not reproduce the observed decrease in the mid-latitude lower stratosphere. Dietmüller et al. (2021) recently investigated 31 CCM simulations and found that none of the model simulations reproduces the coherent negative ozone trends in the tropical and extra-tropical lower stratosphere as shown by recent observations. Instead, most simulations show a dipole pattern with the tropical ozone trend opposite to that in mid-latitudes. These inconsistencies between model simulations and observations imply that dynamical effects on the lower stratospheric ozone changes are still not well understood.

Chemical transport model simulations are ideally suited for interpreting the past ozone changes as well as for quantifying the influence of important physical processes on the ozone variability. However, model-simulated ozone distributions generally show some biases with respect to observation-based datasets due to uncertain photochemical parameters, transport errors and other simplifications of computationally expensive processes (e.g. WMO, 2014, 2018; Dhomse et al., 2018, 2021). The inability of chemical models to simulate the observed lower stratospheric ozone decrease can be largely attributed to the model deficiencies in, for example, transport (Chipperfield et al., 2018; Ball et al., 2018, 2020). Additionally, most observational data records also show large errors due to the measurement technique, instrument limitations or degradation (e.g. Hubert et al., 2016; SPARC, 2019). Hence, comparison between observations and model simulations generally shows time-varying differences. An increase in vertical resolution as well as inclusion of complex chemical and dynamical processes is generally recommended to reduce biases in model-simulated ozone (e.g. Feng et al., 2011; Dhomse et al., 2011).

As CTMs are forced with (re)analysis meteorological fields they are better suited to understand past ozone changes compared to free-running CCMs. Over the time, improvements achieved in meteorological reanalyses such as those from the European Centre for Medium-Range Weather Forecasts (ECMWF) have led to the better representation of stratospheric transport (e.g. Monge-Sanz et al., 2013; Diallo et al., 2021). With the ECMWF fifth generation reanalysis ERA5 (Hersbach et al., 2020) superceding ERA-Interim (Dee et al., 2011), a key question is whether the new reanalysis can improve the simulation performance with respect to the older one when it is used to force CTM simulations (Albergel et al., 2018). It should be noted that there could be inhomogeneities in reanalysis datasets due to changes in available observations assimilated as well as instrument degradation that could introduce spurious transport features (e.g. Schoeberl et al., 2003; Ploeger et al., 2015). Here, we focus on the model performance in interpreting key characteristics of stratospheric ozone using CTM simulations forced by ECMWF ERA-Interim and ERA5 reanalysis datasets. By comparing with observation-based data sets, we evaluate the quality of model simulations and investigate possible reasons for their differences.

The paper is organized as follows. Section 2 describes the CTM simulations forced by ERA-Interim and ERA5 reanalyses, followed by the satellite datasets and regression methods. Section 3 compares the variability and trends in ozone total column and vertical profiles between simulations and observations. The mean age-of-air distributions are also compared and associated with the simulated ozone differences. Section 4 presents our discussion and conclusions.

2 Data and methods

2.1 Model and simulations

Here we use the global off-line 3-D CTM (TOMCAT/SLIMCAT, hereafter TOMCAT) which has been described in detail by Chipperfield (2006). The model contains a detailed description of stratospheric chemistry (e.g. Feng et al., 2011, 2021; Chipperfield et al., 2018), including the concentrations of major ODSs and GHGs (e.g. WMO, 2018), aerosol effects from volcanic eruptions (e.g. Dhomse et al., 2015), and variations in solar forcing (e.g. Dhomse et al., 2016).

ECMWF ERA-Interim reanalyses have been extensively used to drive CTM simulations for multi-annual trend investigations (e.g. Chipperfield et al., 2017; Feng et al., 2021). These reanalyses are based on a coherent assimilation of observations using an atmospheric general circulation model (Dee et al., 2011), covering the period from January 1979 to August 2019. ERA5 is the latest reanalysis product released by ECMWF, to supersede ERA-Interim, and comprehensive account is provided by Hersbach et al. (2020). Both ERA5 and ERA-Interim apply 4-dimensional variational analysis (4D-Var). ERA5 resolves the atmosphere using 137 levels from the surface up to 0.01 hPa (~80 km) with a horizontal spatial resolution of 31 km, while ERA-Interim uses 60 levels from the surface to 0.1 hPa (~65 km) and 80 km for horizontal resolution. ERA5 provides hourly output including information about uncertainties while ERA-Interim provides 6-hourly output.

Here we perform two TOMCAT simulations, A_ERAI and B_ERA5, which are forced with ERA-Interim and ERA5 reanalysis datasets (Dhomse et al., 2019; Feng et al., 2021), respectively. The simulations use identical chemical and dynamical parameters for the whole time period available in ERA-Interim from January 1979 to August 2019. Simulation B_ERA5 uses the corrected ERA5.1 analyses for the period from 2000 to 2006; these have better global-mean temperatures in the lower stratosphere than provided by the original ERA5 product (Simmons et al., 2020). Both TOMCAT simulations are performed at $2.8° \times 2.8°$ horizontal resolution and have 32 hybrid sigma-pressure levels ranging from the surface to about 60 km.

2.2 Satellite datasets

We use the total column ozone (TCO) data from the Copernicus Climate Change Service (hereafter C3S, obtained from https://cds.climate.copernicus.eu/cdsapp#!/dataset/satellite-ozone?tab=overview) for quantification of long-term variability

https://doi.org/10.5194/acp-2022-182
Preprint. Discussion started: 7 April 2022

Atmospheric Chemistry and Physics Discussions

and trends. This monthly mean gridded dataset is created by combining total ozone data from 15 satellite sensors, including the Global Ozone Monitoring Experiment (GOME, 1995-2011), Scanning Imaging Absorption Spectrometer for Atmospheric CHartographY (SCIAMACHY, 2002-2012), Ozone Monitoring Instrument (OMI, 2004-present), GOME-2A/B (2007-present), Backscatter Ultraviolet Radiometer (BUV-Nimbus4, 1970-1980), Total Ozone Mapping Spectrometer (TOMS-EP, 1996-2006), Solar Backscatter Ultraviolet Radiometer (SBUV-9, -11, -14, -16, -17, -18, -19, 1985-present) and Ozone Mapping and Profiler Suite (OMPS, 2012-present). This merged product spans from 1970 to present and the horizontal resolution after January 1979 is 0.5 ° × 0.5 °. The long-term stability of the total column product is below the 1%/decade level. Systematic and random errors in this data are below 2% and 3-4%, respectively, which makes it suited for long-term trend analysis. Sofieva et al. (2017) and Steinbrecht et al. (2017) evaluated the ozone trends and reported that they are in agreement with those presented in WMO (2014). Li et al. (2020) confirmed that there is no long-term drift in the C3S data and showed the differences between C3S and the SBUV satellite data are less than 2-3% throughout the record 1979-2017.

The Stratospheric Water and OzOne Satellite Homogenized (SWOOSH, obtained from https://csl.noaa.gov/groups/csl8/swoosh/) dataset is used to evaluate our simulated ozone profiles. SWOOSH includes a merged record of stratospheric ozone and water vapour measurements, comprised of data from the Stratospheric Aerosol and Gas Experiment (SAGE-II/III), Upper Atmospheric Research Satellite Halogen Occultation Experiment (UARS HALOE), UARS Microwave Limb Sounder (MLS), and Aura MLS instruments (Davis et al., 2016 and references therein). The measured values are homogenized by applying the corrections calculated from data collected during the overlapping time periods of the instrument. The merged SWOOSH record spans from 1984 to present, and consists of monthly mean zonal-mean ozone values on pressure levels from 316 to 1 hPa (31 levels). Comparisons between the SWOOSH merged product and independent ground-based measurements (e.g. Hubert et al., 2016) and satellite data sets (e.g. Harris et al., 2015) confirm the long-term stability of the SWOOSH ozone product.

2.3 Regression methods

Multi-variate linear regression models (MLR) are widely used to assess long-term ozone trends (e.g. Reinsel et al., 2002; Dhomse et al., 2006; Chehade et al., 2014; Steibrecht et al., 2017; Li et al., 2020). Here we use a piecewise linear trend (PWLT)-based regression model to analyse the robustness of the depletion and recovery trends in total ozone column and vertical ozone profiles before and after the peak stratospheric halogen loading in 1997. Traditional explanatory proxies, including the solar flux for the 11-year solar cycle, quasi-biennial oscillation (QBO) at 30 hPa and 10 hPa (QBO30 and QBO10), El-Nino Southern Oscillation (ENSO), stratospheric aerosol loading from volcanic eruptions and Arctic Oscillation (AO) or Antarctic Oscillation (AAO) index, are considered to account for influence of chemical and dynamical processes (e.g. Solomon et al., 1996; Randel and Wu, 2007; Fioletov, 2009 and references therein). The time series of the total ozone or vertically resolved ozone anomalies ($Y(\mathrm{t})$) are constructed as a linear sum of trends and explanatory-variable time series as follows:

https://doi.org/10.5194/acp-2022-182
Preprint. Discussion started: 7 April 2022

$$Y(\mathrm{t}) = C_0 + C_1 \cdot t_1 + C_2 \cdot t_2 + \sum C_i \cdot X_i\,(\mathrm{t}) + \varepsilon(t), \tag{1}$$

where t is the time (years or months) during the period 1979-2018, C_0 is a constant for the long-term average, C_1 and C_2 are coefficients of the linear trends (Trend1 and Trend2) in the periods 1979 (1984)-1997 and 1998-2018, C_i represents the time-dependent regression coefficient of each proxy Xi (Solar, QBO30, QBO10, ENSO, Aerosol and AO/AAO) and ε is the residual term.

3 Results

In Section 3.1, we apply the PWLT-based regression model to the December-January-February (DJF) and June-July-August (JJA) mean TCO to determine the wintertime and summertime total ozone variations in C3S and simulations A_ERAI and B_ERA5 over the period 1979-2018. The proxies are also averaged for DJF and JJA seasons. Cross correlations between each proxy are less than 0.3 except for Solar and AO (0.43), ENSO and Aerosol (0.37), but here we assume two natural proxies (solar and stratospheric aerosol variations) are independent from internal climate variability or teleconnection patterns (AO and ENSO). When we apply the regression model to the vertically resolved ozone anomalies (Section 3.2) to obtain the trend distribution in the periods 1984-1997 and 1998-2018, the remaining residuals are not normally distributed. Hence, the Cochrane-Orcutt transformation with a time lag of one month is applied to the regression equation to avoid non-negligible auto-correlation in the residuals (e.g. Reinsel et al., 2002; Dhomse et al., 2006). In this case, cross correlations between each proxy are less than 0.3. The ozone trend profiles from 147 hPa to 1 hPa (100 hPa to 1 hPa for the tropical region) are calculated with the coefficients referenced to the ozone values at different pressure levels.

3.1 Variability and trends in total column ozone

To evaluate the performance of model simulations compared to observations, we first look at the characteristics of total column ozone (TCO) anomalies in different latitude regions over the extended time period 1979-2019 (August). Anomalies are calculated by subtracting the long-term monthly average from each monthly mean value.

https://doi.org/10.5194/acp-2022-182
Preprint. Discussion started: 7 April 2022

Atmospheric Chemistry and Physics
Discussions

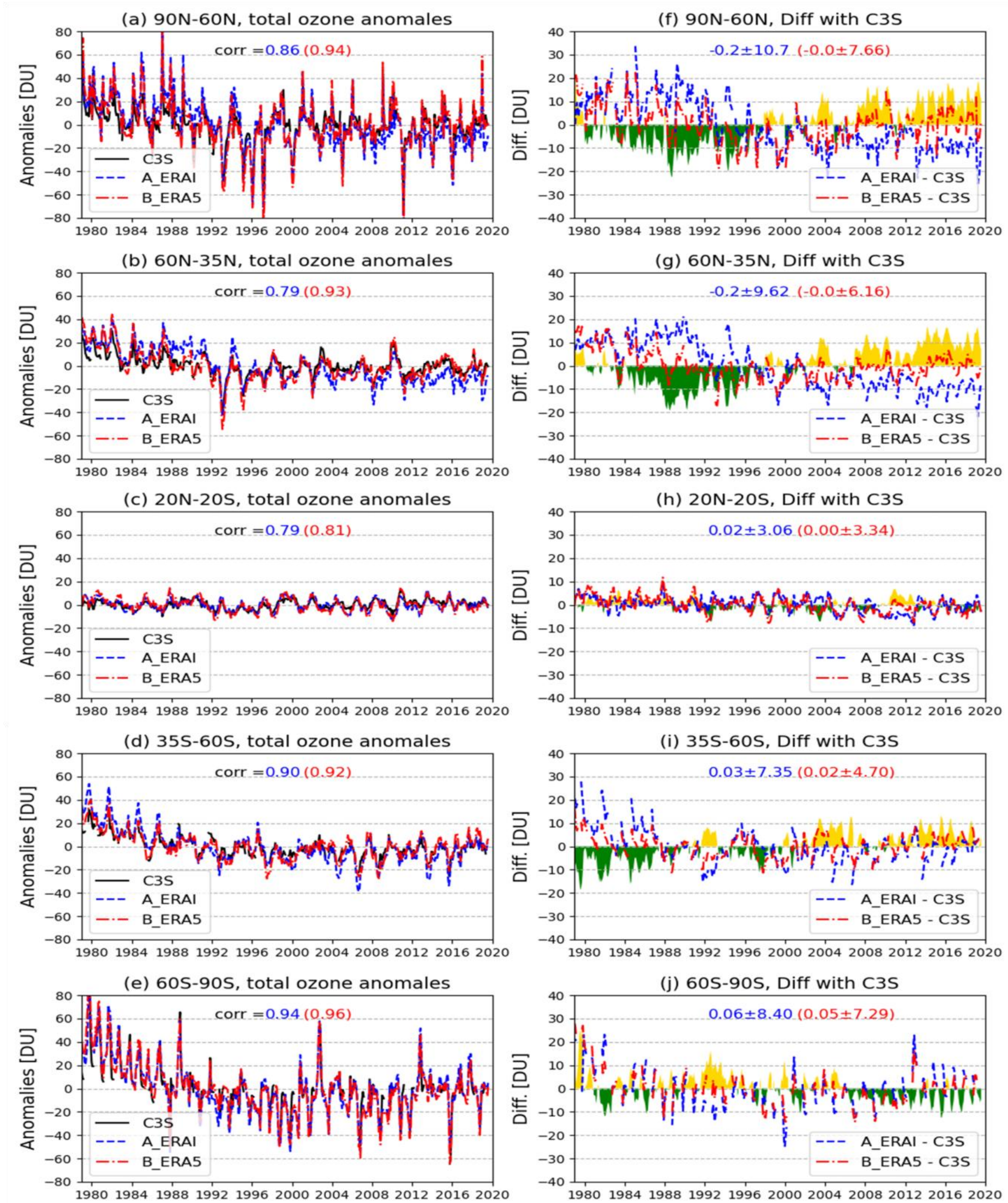

Figure 1: (Left panels a-e) Total column ozone (TCO) anomalies (DU) derived from C3S (black solid line) and TOMCAT simulations A_ERAI (blue dashed line) and B_ERA5 (red dash-dot line) over 1979-2019 (August) for five latitude regions: 90 °N-60 °N, 60 °N-35 °N, 20 °N-20 °S, 35 °S-60 °S and 60 °S-90 °S. (Right panels f-j) Absolute differences in TCO between each simulation and C3S (blue dashed line for A_ERAI - C3S and red for B_ERA5 - C3S) as well as

https://doi.org/10.5194/acp-2022-182
Preprint. Discussion started: 7 April 2022

Atmospheric Chemistry and Physics
Discussions

between the two simulations (B_ERA5 - A_ERAI, shaded with green colour for B_ERA5 < A_ERAI and yellow for B_ERA5 > A_ERAI). Correlation coefficients and TCO differences with standard deviations between simulation A_ERAI (B_ERA5) and C3S are shown with blue (red) text.

Figures 1a-e (left column) show the monthly mean TCO anomalies obtained from merged C3S and TOMCAT simulations, A_ERAI and B_ERA5, over 1979-2019 (August) for the NH high-latitudes (90°N-60°N), mid-latitudes (60°N-35°N), tropics (20°N-20°S), SH mid-latitudes (35°S-60°S) and SH high-latitudes (60°S-90°S). The absolute differences of the climatological anomalies between each simulation and C3S, as well as between the two model simulations (B_ERA5 - A_ERAI), are also shown in **Figures 1f-j** (right column). Overall, both model simulations are able to capture the temporal characteristics in ozone variations relative to C3S very well, confirming the realistic representation of important chemical and dynamical processes in TOMCAT. However, the magnitude and structure of the inter-annual total ozone anomalies show different aspects of differences between two reanalysis data sets in different latitude regions. For example, correlation analysis between simulated and C3S TCO anomalies shows that B_ERA5 is better correlated to C3S than A_ERAI for most latitude regions. In particular, in the NH mid-latitude region B_ERA5 shows much better correlation (0.93) with C3S than A_ERAI (0.79), meaning that B_ERA5 anomalies track observed anomalies better than A_ERAI, especially during 1980s. An interesting feature in **Figures 1f-g** is that simulations A_ERAI and B_ERA5 show significant differences at NH mid-high latitudes. The comparison also shows that before 1998 anomalies from B_ERA5 are relatively smaller than from A_ERAI (up to ~ -20 DU biases – shaded green regions) but are larger during later years (up to ~ +20 DU biases – shaded yellow regions). The better agreement between B_ERA5 and C3S, compared to the larger biases between A_ERAI and C3S especially, in the NH mid-high-latitude regions could be due to possible deficiencies such as representation of dynamical processes in the ERA-Interim reanalyses.

https://doi.org/10.5194/acp-2022-182
Preprint. Discussion started: 7 April 2022

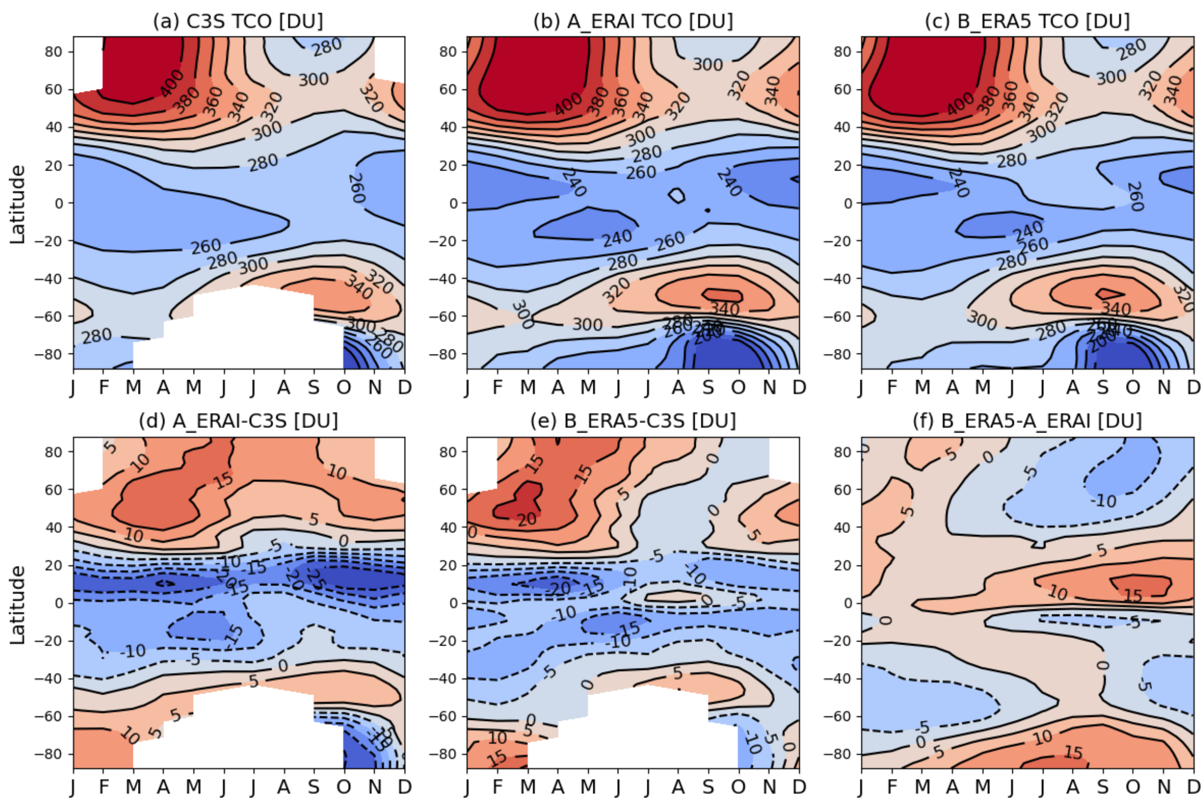

Figure 2: Zonal and monthly mean TCO (DU) climatology over the period 1979-2018 based on (a) C3S and two model simulations (b) A_ERAI and (c) B_ERA5. The absolute differences between each simulation and C3S, as well as between the two simulations, are shown in (d) A_ERAI - C3S, (e) B_ERA5 - C3S and (f) B_ERA5 - A_ERAI, respectively.

Figure 2 compares the C3S TCO with A_ERAI and B_ERA5 simulations over the period 1979-2018 to examine the climatological seasonal cycle characteristics of TCO. As expected, both model simulations reproduce the major seasonal characteristics of the zonal mean distribution of C3S TCO (**Figures 2a-c**). Differences between the model simulations and C3S (**Figures 2d-e**) show that TCO in the tropics (especially north of the Equator) is underestimated in both simulations compared to C3S. Compared to the large negative biases (up to ~30 DU) seen in A_ERAI, TCO from B_ERA5 exhibits relatively smaller negative biases (< ~20 DU) in the tropics. In NH mid-high latitudes, A_ERAI overestimates the observed C3S TCO across all seasons, while B_ERA5 shows larger positive biases (more than 15 DU) during NH winter-spring seasons but negligible biases during summer-autumn seasons. The comparison in **Figure 2f** shows that B_ERA5 exhibits positive TCO differences at mid-high latitudes during winter-spring seasons in both hemispheres. This characteristic points to potential differences in the representation of tropics-to-mid-high-latitude ozone transport via the meridional circulation (the Brewer-Dobson circulation (BDC)) between the two reanalysis data sets. For example, positive differences in **Figure 2f** during NH winter-spring seasons, and negative differences during summer-autumn seasons, indicate that on average

https://doi.org/10.5194/acp-2022-182
Preprint. Discussion started: 7 April 2022

wintertime ozone build-up and summertime ozone losses are significantly different between two model simulations. Also, during SH spring (September-October-November) slightly larger TCO in the tropics and smaller values at mid-latitudes in B_ERA5 indicate weaker ozone transport in ERA5. At the same time, larger TCO values in the SH polar cap during JJA (June-July-August) may indicate more mixing near the edge of the Antarctic polar vortex.

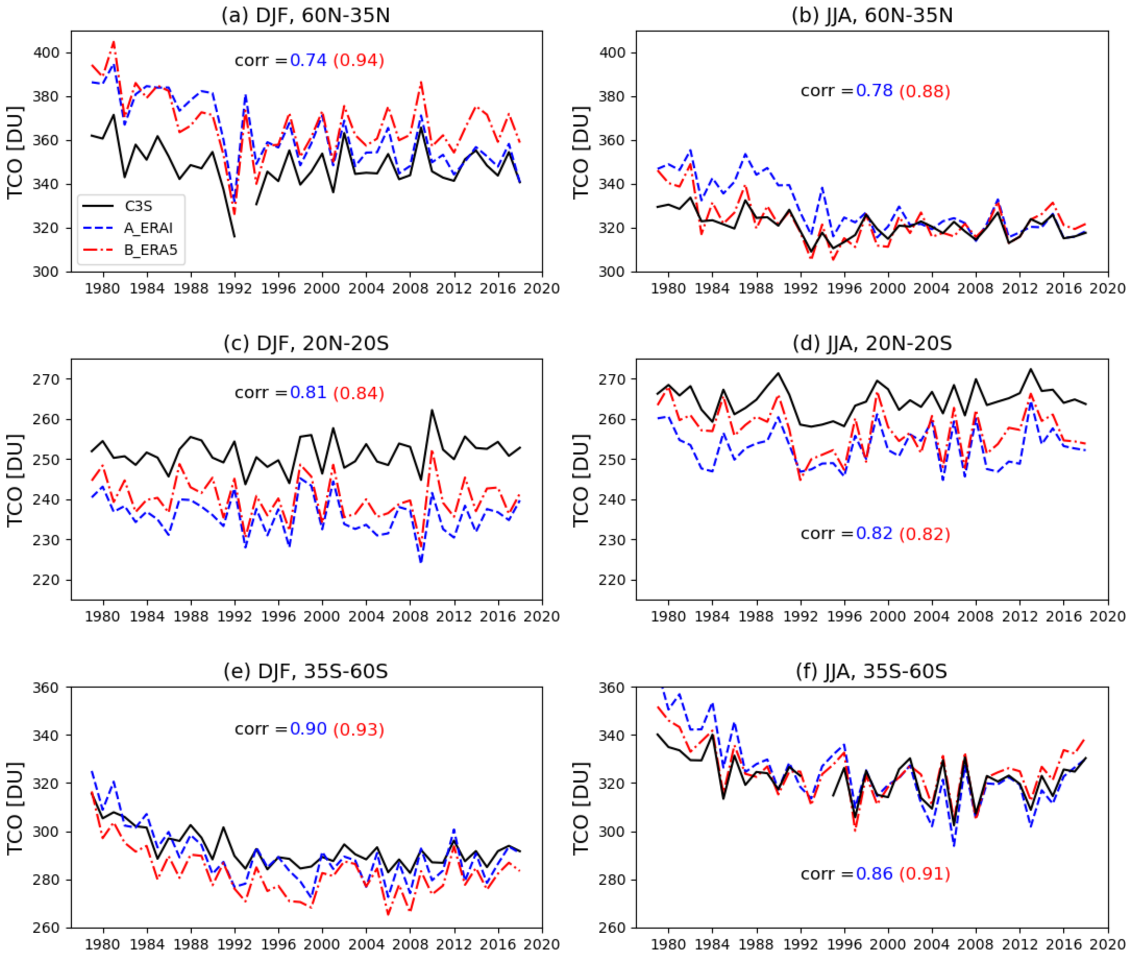

Figure 3: December-January-February (DJF) and June-July-August (JJA) mean TCO (DU) for the period 1979-2018 from C3S (black solid line), A_ERAI (blue dashed line), and B_ERA5 (red dash-dot line) averaged over the latitude bands (a, b) 60°N-35°N, (c, d) 20°N-20°S and (e, f) 35°S-60°S. Correlation coefficients between simulation A_ERAI (B_ERA5) and C3S are shown in each panel with blue (red) text.

Figure 3 compares the seasonal evolution of DJF and JJA mean TCO averaged over 60°N-35°N, 20°N-20°S and 35°S-60°S from C3S, A_ERAI and B_ERA5. Both CTM simulations capture the observed seasonal characteristics of TCO variations averaged across all latitude bands considered here, in line with the results in **Figure 2**. Stratospheric transport is dominant in winter leading a steady build-up in mid-high latitude TCO in both hemispheres, while in summertime there is a steady decline due to photochemical loss (e.g. Fioletov and Shepherd, 2003; Tegtmeier et al., 2008). As noted earlier, both

https://doi.org/10.5194/acp-2022-182
Preprint. Discussion started: 7 April 2022

Atmospheric Chemistry and Physics Discussions

model simulations A_ERAI and B_ERA5 underestimate the observed DJF and JJA mean total ozone variability in the tropics, indicating either or both models have weaker ozone production and/or stronger ozone transport to mid-high latitudes. Focusing on the mid-latitudes (**Figures 2a-2b and 2e-2f**), the TCO in A_ERAI is more comparable with C3S in the SH mid-latitude band but is overestimated in the NH mid-latitudes, especially in the period until 1992. B_ERA5 overestimates the observed DJF mean TCO in the NH mid-latitudes while it underestimates it in the SH mid-latitudes. In JJA, B_ERA5 agrees better with C3S in both hemisphere mid-latitudes, except for the overestimation in the beginning and end years. Consistent with the results of correlation analysis shown in **Figure 1,** which is based on monthly TCO anomalies, both simulations A_ERAI and B_ERA5 are better correlated with C3S in the SH than in the tropical and NH mid-latitude bands. Overall simulation B_ERA5 shows relatively better correlation with C3S in both seasons for all latitude bands.

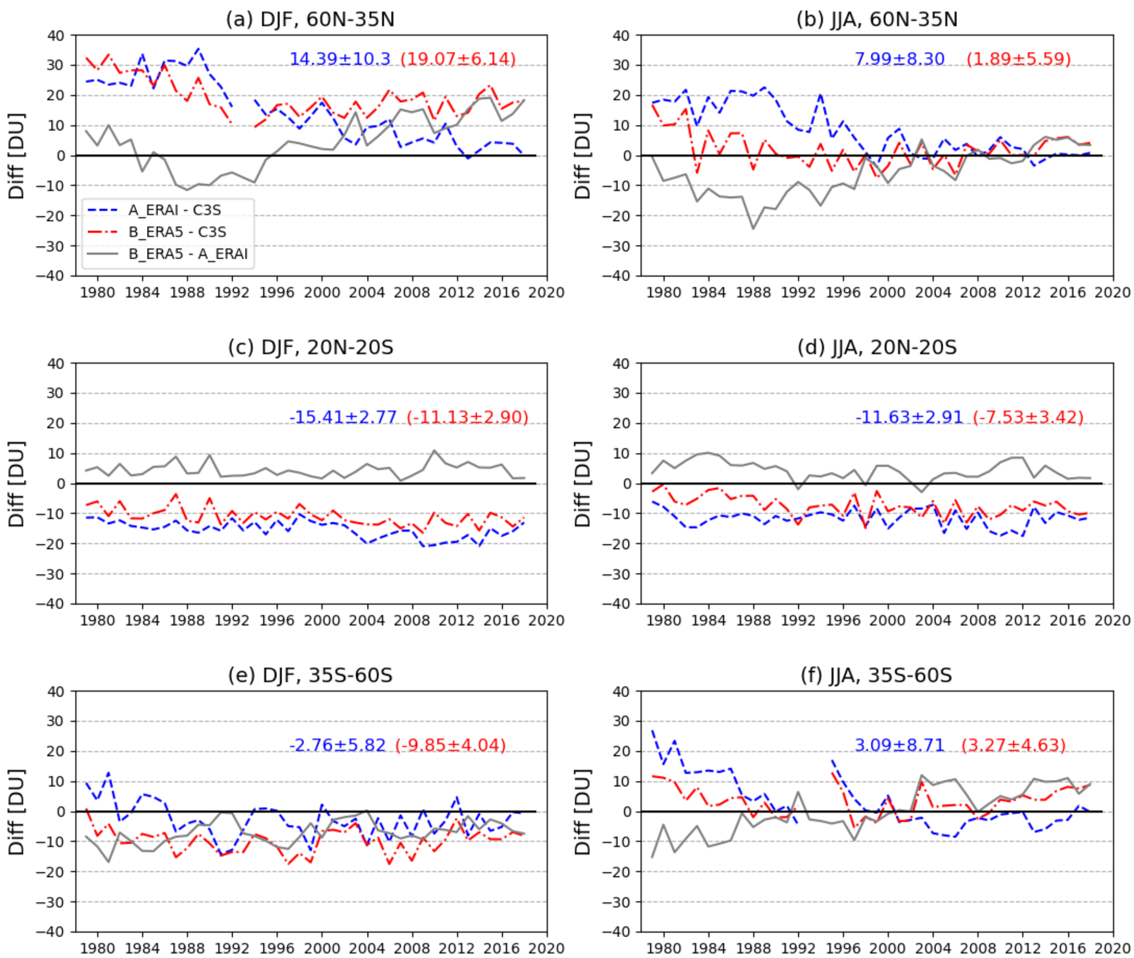

Figure 4: Differences in total column ozone (DU) between two model simulations and C3S (blue dashed line for A_ERAI - C3S and red dash-dot line for B_ERA5 - C3S) as well as between two simulations (grey solid line for B_ERA5 - A_ERAI). Average total column differences are shown for (a, b) 60 °N-35 °N, (c, d) 20 °N-20 °S and (e, f) 35 °S-60 °S for December-January-February (DJF, left panel) and June-July-August (JJA, right panel) seasons. The

https://doi.org/10.5194/acp-2022-182
Preprint. Discussion started: 7 April 2022

absolute differences with the standard deviations averaged over the whole period between simulation A_ERAI (B_ERA5) and C3S are presented in blue (red) text.

The DJF and JJA mean TCO differences between the model simulations and C3S over the period 1979-2018 are compared in **Figure 4**. At NH mid-latitudes (60 °N-35 °N), A_ERAI initially shows positive biases compared to C3S of 14.39±10.30 DU in DJF and 7.99±8.43 DU in JJA, which decreases to near-zero values with time. In contrast, B_ERA5 shows relatively steady positive biases (19.07±6.14 DU) in DJF and near-zero biases (1.89±5.59 DU) in JJA. As a result, the difference between two model simulations (B_ERA5 - A_ERAI) increases with time in both seasons. In the tropics (20 °N-20 °S), both simulations underestimate the DJF and JJA mean TCO compared to C3S, with larger negative biases seen in A_ERAI. The differences between the two simulations (B_ERA5 - A_ERAI) remain within +10 DU in both DJF and JJA timeseries. At SH mid-latitudes (35 °S-60 °S), both A_ERAI and B_ERA5 underestimate the DJF mean TCO in C3S but with larger negative biases in B_ERA5 (-9.85±4.04 DU) than in A_ERAI (-2.76±5.82 DU). In JJA, TCO differences between A_ERAI and C3S change from positive to negative around the late 1990s, while B_ERA5 shows mostly positive biases (3.27±4.63 DU) compared to C3S. Thus, their difference increases with time and changes from negative to positive in JJA. As shown in **Figures 4a** and **4e** there are larger biases in B_ERA5 than in A_ERAI while the correlation coefficients between B_ERA5 and C3S are higher than A_ERAI (as shown in **Figure 3**), which suggests that there may exist some unrealistic annual variability in A_ERAI.

To gain better insight about the implications to the ozone trend estimation due to differences discussed above, we apply the PWLT-based multi-variate linear regression model to the DJF and JJA mean TCO time series to determine the long-term (1979-2018) ozone trends and changes over 60°N-35°N, 20°N-20°S and 35°S-60°S. The regression model used here is identical to that used in Li et al. (2020), except for the different explanatory variables considered for different latitude bands. **Table 1** lists the determination coefficients (R-squared) based on the PWLT regression model for DJF (JJA) mean TCO time series from C3S, A_ERAI and B_ERA5 over the 60°N-35°N, 20°N-20°S and 35°S-60°S regions.

Table 1: Determination coefficients (R-squared) based on PWLT regression model for DJF (JJA) mean TCO time series from C3S, A_ERAI and B_ERA5 over 60 °N-35 °N, 20 °N-20 °S and 35 °S-60 °S regions.

Latitude bands	C3S DJF (JJA)	A_ERAI DJF (JJA)	B_ERA5 DJF (JJA)
60°N-35°N	0.78 (0.66)	0.86(0.82)	0.83 (0.79)
20°N-20°S	0.75 (0.68)	0.79 (0.73)	0.74 (0.73)
35°S-60°S	0.84 (0.65)	0.85 (0.79)	0.82 (0.71)

https://doi.org/10.5194/acp-2022-182
Preprint. Discussion started: 7 April 2022

Atmospheric Chemistry and Physics
Discussions

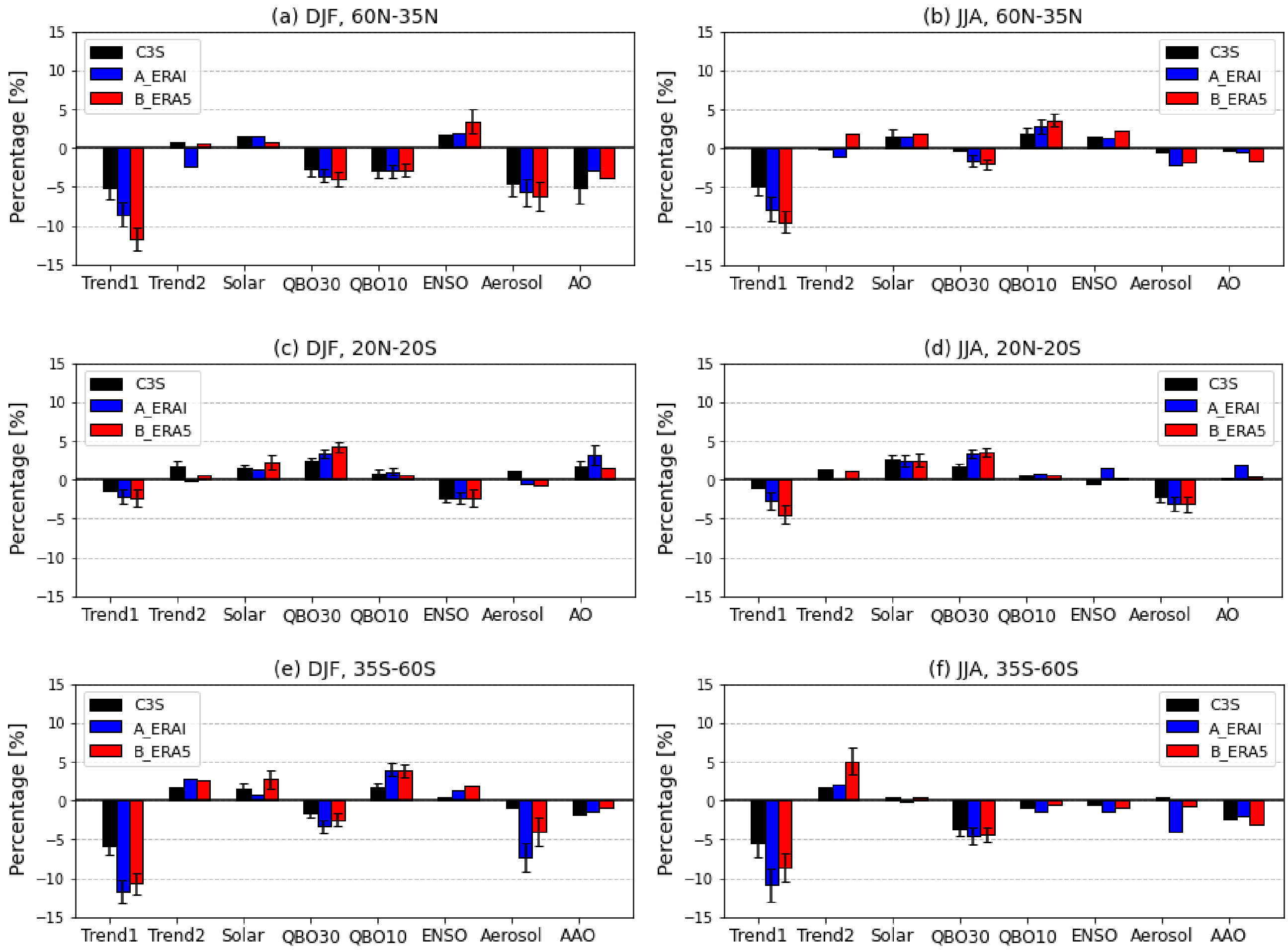

Figure 5: Peak contributions (in %) from piecewise linear trend and explanatory variable terms (see equation (1)) to the total ozone column variability during DJF and JJA for (a, b) 60 °N-35 °N, (c, d) 20 °N-20 °S and (e, f) 35 °S-60 °S for C3S, A_ERAI and B_ERA5 during 1979-2018. Error bars indicate the confidence bounds at the 95% statistical significance level quantified by ± 2 standard deviations (σ).

The percentage ozone changes derived from peak contributions of different proxies ($\frac{max-min}{mean} \times 100\%$) are shown in **Figure 5**. Error bars indicate the confidence bounds at the 95% statistical significance level quantified by ± 2 standard deviations (σ), and the negative and positive patterns come from fitting coefficients. As expected, the regression models for C3S and CTM simulations show negative trends at all latitude bands considered here before 1998 (Trend1), with more significant decreases at NH and SH mid-latitude bands for the simulations than C3S.

The recovery since 1998 (Trend2) from C3S is quite different to that from the simulations in terms of its magnitude and significance. C3S shows weak recovery for all three latitude bands, with a significant recovery trend in DJF for the tropical region. Simulation A_ERAI shows negligible but positive trends in the tropical and SH mid-latitude regions, but they are negative in both DJF and JJA at NH mid-latitudes. In contrast, B_ERA5 shows positive trends for all three latitude bands

https://doi.org/10.5194/acp-2022-182
Preprint. Discussion started: 7 April 2022

Atmospheric Chemistry and Physics
Discussions

that are larger than 2-σ variance in the SH mid-latitudes. These differences in ozone recovery can be linked to the differences between ERA5 and ERA-Interim forcing fields (such as trends in stratospheric transport processes) used in model simulations.

The differences in the proxy contributions for the DJF and JJA seasons are consistent with our understanding that total ozone variability is dominated by different processes in winter and summer. We also find slight differences in proxy contributions to the total ozone variability from C3S, A_ERAI and B_ERA5, but to a large extent contributions from the solar cycle, QBO, ENSO, aerosol and AO/AAO in the ozone variability are somewhat similar. For example, positive QBO anomalies in the tropics and negative anomalies in the subtropical regions are associated with the QBO phase change from the equator to the subtropics. Negative AO (AAO) anomalies lead to enhanced ozone at the northern (southern) mid-latitudes (e.g. Chehade et al., 2014).

3.2 Variability and trends in ozone profiles

We now compare ozone profiles from model simulations and SWOOSH dataset. **Figure 6** shows vertical profiles of ozone averaged over 60°N-35°N, 20°N-20°S and 35°S-60°S latitude bins, along with the relative differences for each model simulation with respect to SWOOSH for the whole time period (1984-2018) as well as for DJF and JJA seasons. In all cases, both A_ERAI and B_ERA5 underestimate upper stratospheric ozone concentrations while overestimate the middle and lower stratospheric ozone concentrations to varying degrees (e.g. Dhomse et al., 2021).

Overall, simulation B_ERA5 shows larger negative biases in the upper stratosphere (up to ~ -10% at 3 hPa) than does A_ERAI. In the middle stratosphere (32-10 hPa), both simulations are in good agreement with each other. The biases between model simulations and SWOOSH in the lower stratosphere change with latitude bands and seasons. In the tropical lower stratosphere (~80 hPa), B_ERA5 shows larger (~ +50%) biases than those in A_ERAI (~ +27%) for both DJF and JJA seasons. Although B_ERA5 shows better correlation with the observed tropical TCO and smaller differences than A_ERAI does, the comparison in tropical ozone profiles indicates that w. r. t. SWOOSH, B_ERA5 has larger biases in both the upper and lower stratosphere. In the NH mid-latitude lower stratosphere (~100 hPa), B_ERA5 exhibits slightly more positive biases from SWOOSH in DJF (boreal winter) but smaller biases in JJA than A_ERAI does. In the SH mid-latitude lower stratosphere, A_ERAI shows larger biases in DJF (austral summer) but the biases in JJA for both simulations are comparable. The comparison of ozone changes between two simulations indicates that their differences in the lower stratosphere largely contribute to their differences in TCO. In the lower stratosphere ozone is long-lived and under dynamical control, indicating the effects of changes in background meteorological forcing fields on simulated lower stratospheric ozone.

https://doi.org/10.5194/acp-2022-182
Preprint. Discussion started: 7 April 2022

Atmospheric Chemistry and Physics Discussions

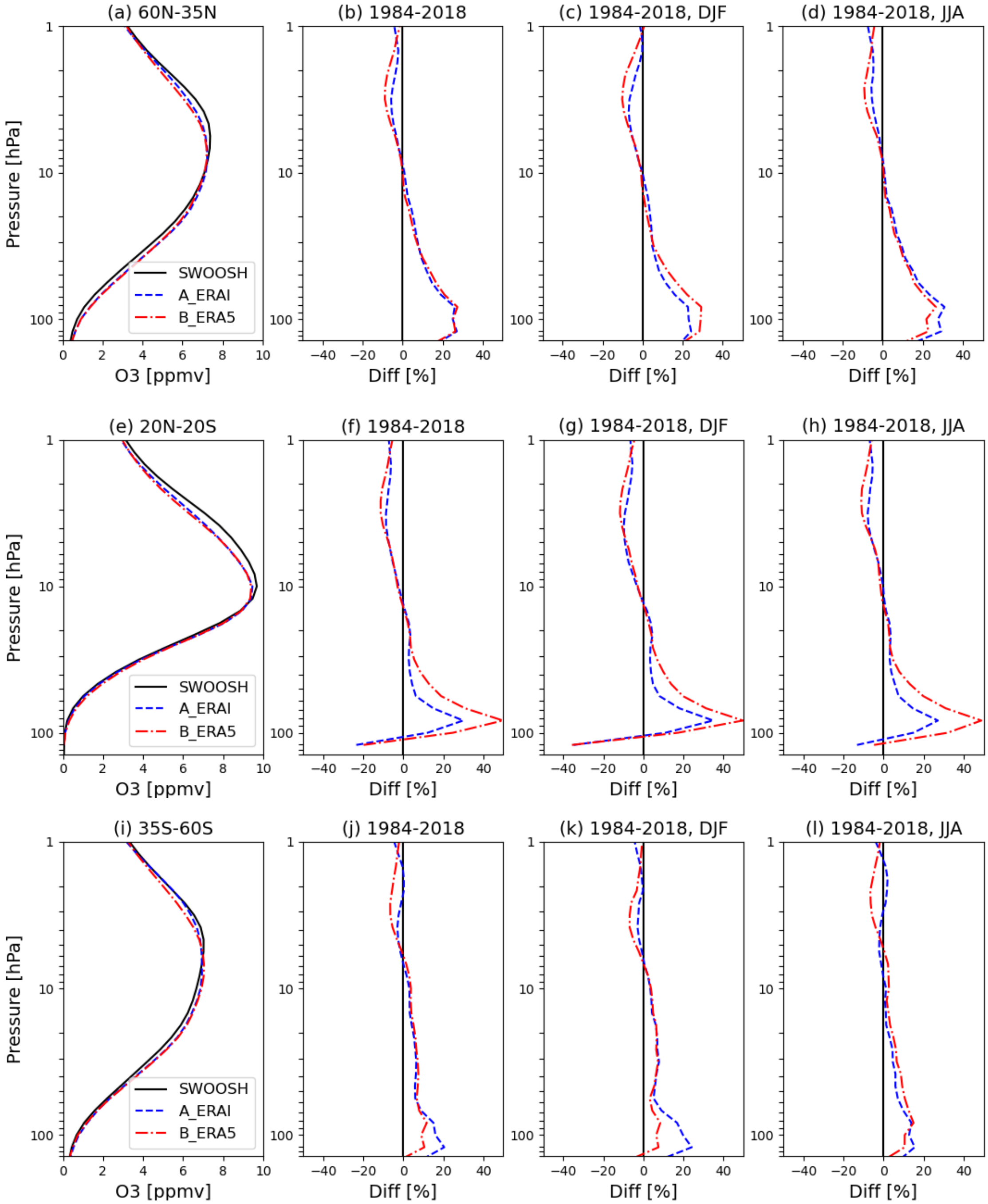

335 **Figure 6: Averaged vertical ozone profiles from SWOOSH (black solid line), A_ERAI (blue dashed line) and B_ERA5 (red dash-dot line) for (a-d) 60°N-35°N, (e-h) 20°N-20°S, and (i-l) 35°S-60°S (1984-2018). Relative differences (%) referencing each simulation to SWOOSH averaged in the whole time period as well as DJF and JJA seasons are shown in the three right-hand columns for comparison.**

https://doi.org/10.5194/acp-2022-182
Preprint. Discussion started: 7 April 2022

Atmospheric Chemistry and Physics
Discussions

After analysing biases in mean ozone profiles, we diagnose time-dependent differences between two simulations. **Figure 7** shows percentage differences between A_ERAI and B_ERA5 for five latitude bands from 147 hPa to 1 hPa. The positive differences in the upper stratosphere after 1998 for all latitude regions can clearly be seen, which means that upper stratospheric anomalies in simulation B_ERA5 are overestimated compared to A_ERAI despite the overall slight underestimation seen in **Figure 6**. In the NH mid-high latitudes, the relative differences in the lower stratospheric ozone between the two simulations (B_ERA5-A_ERAI) also change from negative before 1998 to positive afterwards. These differences in the NH stratosphere (when integrated) are consistent with the characteristics seen in TCO anomalies as shown in **Figures 1f-g**. In the tropical lower stratosphere, B_ERA5 overestimates the ozone anomalies in A_ERAI during the periods 1979-1991 and 2010-2016, and underestimates in other periods. The situation in the SH mid-latitude lower stratosphere is similar to that in the NH mid-latitude where the biases between two simulations change from negative to positive around 2000, while it is not the case in the SH polar region. The comparison of the CTM simulations with SWOOSH (see the supplementary **Figures S1** and **S2**) confirms that the observed stratospheric ozone concentrations in the NH and SH mid-latitude regions are overall overestimated by A_ERAI for earlier years (1984-1991) while they are overestimated by B_ERA5 during the later period 2006-2019 (August).

https://doi.org/10.5194/acp-2022-182
Preprint. Discussion started: 7 April 2022

Atmospheric Chemistry and Physics Discussions

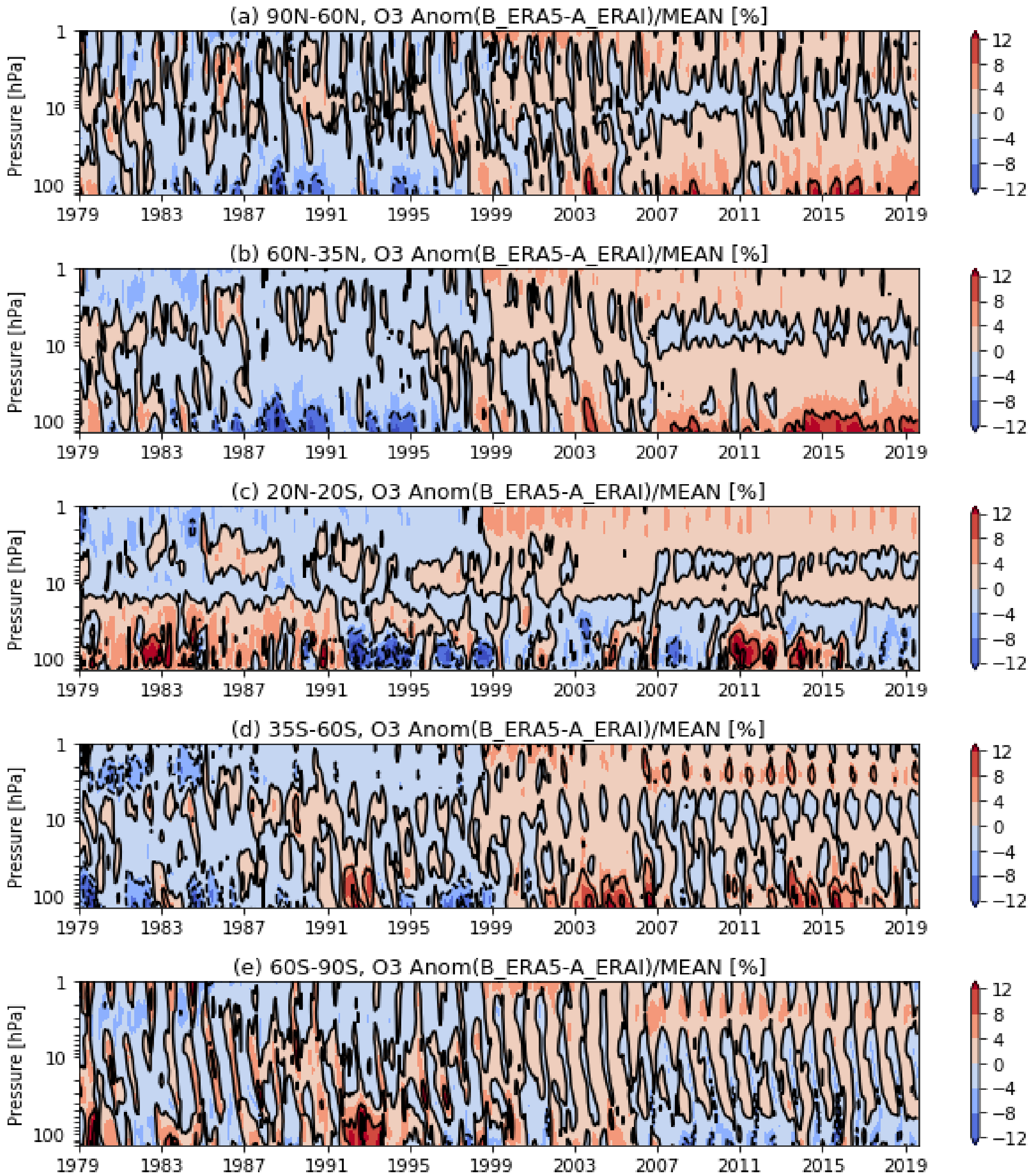

355 **Figure 7: Pressure-time evolution of the percentage differences in ozone anomalies between A_ERAI and B_ERA5 over 1979-2019 (August) for different latitude regions (a) 90 °N-60 °N, (b) 60 °N-35 °N, (c) 20 °N-20 °S, (d) 35 °S-60 °S and (e) 60 °S-90 °S.**

https://doi.org/10.5194/acp-2022-182
Preprint. Discussion started: 7 April 2022

Atmospheric Chemistry and Physics
Discussions

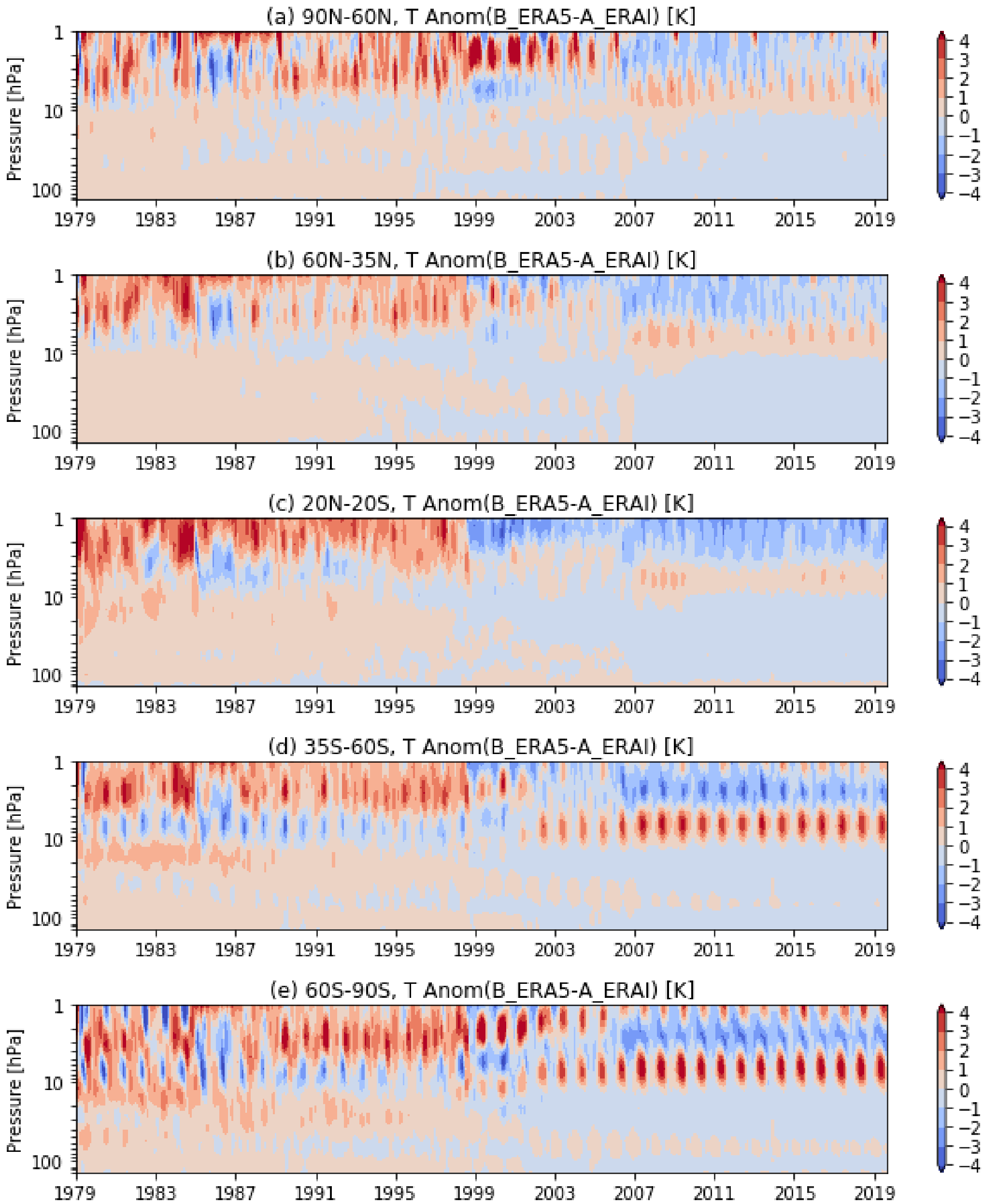

Figure 8: Similar to Figure 7 but for differences in temperature anomalies (K) between A_ERAI and B_ERA5 (B_ERA5- A_ERAI). Note the simulation B_ERA5 uses ERA5.1 reanalysis for the period 2000-2006.

360 As ozone loss reactions are temperature dependent (e.g. Randel and Cobb, 1994; Douglass et al., 2012), in **Figure 8** we compare the temperature anomalies between A_ERAI and B_ERA5 to account for the relative differences in ozone anomalies in a similar fashion to **Figure 7**. Large biases in temperature anomalies between two simulations (B_ERA5-A_ERAI) appear in the upper stratosphere for all latitude regions until around 1998, confirming that some of the

https://doi.org/10.5194/acp-2022-182
Preprint. Discussion started: 7 April 2022

inhomogeneities seen in ERA-Interim upper stratospheric temperatures (Dhomse et al., 2011; McLandress et al., 2014) associated with changes in assimilation of Microwave Limb Sounder data have been corrected in ERA5. Besides, ERA5 has a higher top layer up to ~80 km with finer vertical resolution in the upper stratosphere than ERA-Interim which only extends up to ~65 km. The update in the radiation scheme and the improvement in the wind extrapolation scheme in ERA5 also mitigates erroneous temperatures compared to ERA-Interim (Hersbach, 2020 and references therein). Thus, the differences in the upper stratospheric temperatures from the reanalysis data sets drive the differences in ozone anomalies in this region. In the lower stratosphere, however, temperature differences between the two simulations are relatively small and similar for all latitude bands, which cannot explain the differences in the lower stratospheric ozone anomalies. This corroborates the fact the ozone variability in the lower stratosphere depends on a much more complex combination of factors than that in the upper stratosphere.

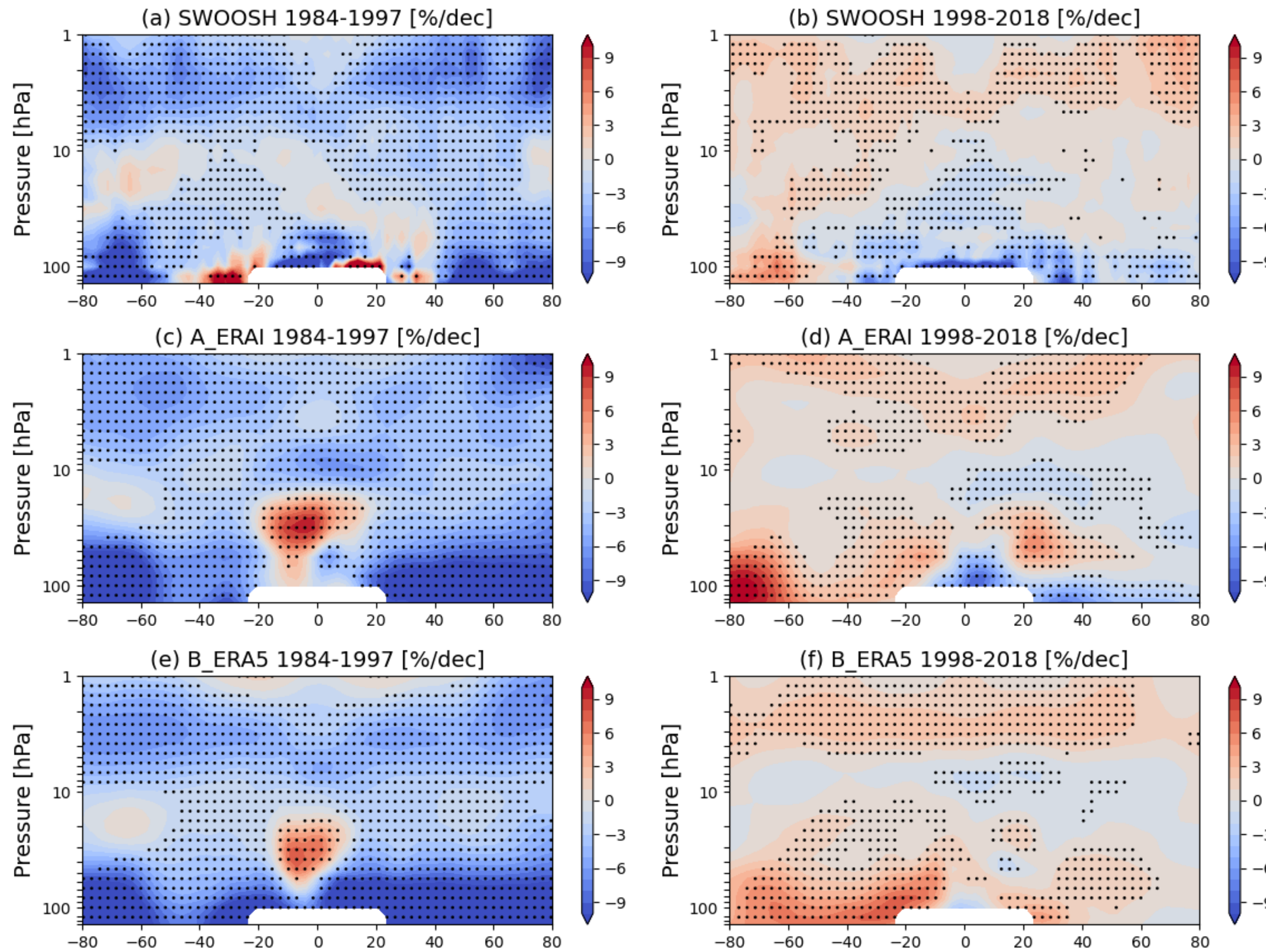

Figure 9: Pressure-latitude cross sections of the piecewise linear trends of ozone anomalies (%/decade) over the periods 1984-1997 and 1998-2018 for (a, b) SWOOSH, (c, d) A_ERAI and (e, f) B_ERA5, respectively. Stippled regions indicate where the trends are statistically significant at 95% level of confidence.

https://doi.org/10.5194/acp-2022-182
Preprint. Discussion started: 7 April 2022

Figure 9 shows the PWLT trends for the zonal mean ozone anomalies over the periods 1984-1997 and 1998-2018 obtained from SWOOSH, A_ERAI and B_ERA5 simulations. Both A_ERAI and B_ERA5 reproduce the decreasing ozone trends before 1998, with some exceptions such as the inconsistent positive trends in the tropical region and the overestimated decline in the extratropical lower stratosphere relative to SWOOSH results. The significant inconsistencies in the tropical region suggest that both model simulations are unable to reproduce SWOOSH type variations in the tropical lower stratosphere. It is also important to note that much smaller ozone concentrations in this region means larger retrieval errors for satellite measurements that are used in SWOOSH data set. Both simulations also overestimate the downward trend in the extratropical lower stratosphere that partly explains the overestimated decline in simulated TCO (Trend1) in the NH and SH mid-latitude regions (**Figure 5**). For the later period (1998-2018), both simulations show the increasing trends in the upper stratosphere that are consistent with SWOOSH-derived trends. Harris et al. (2015) argued that this increase is associated with stratospheric cooling and an almost linear decrease in stratospheric chlorine loading. In the lower stratosphere, both SWOOSH and A_ERAI show negative trends in the tropical and NH extratropical regions, while B_ERA5 shows increasing trends throughout almost the whole extratropical region. Similar to the increasing mid-latitude trends found in most CCMs (Ball et al., 2020; Dietmüller et al., 2021), the increasing NH mid-latitude trends in B_ERA5 indicate possible discrepancies in ERA5 dynamics especially in the lower stratosphere.

Zonally averaged linear trends for 60°N-35°N, 20°N-20°S and 35°S-60°S from SWOOSH, A_ERAI and B_ERA5 are shown in the supplementary **Figure S3** to quantitatively describe the long-term changes over the periods 1984-1997 and 1998-2018. During the period 1984-1997, SWOOSH ozone data show a consistent decrease in the whole stratosphere across all three latitude bands considered here. Simulations A_ERAI and B_ERA5 are able to reproduce negative ozone trends, especially in the SH middle and upper stratosphere. However, both simulations overestimate the decline in the mid-latitude lower stratosphere, with trends varying from -15±1.9% to -7.8±1.4% per decade at 100 hPa. They even show opposite increasing ozone in the tropical low-middle stratosphere between 15 and 50 hPa. During 1998-2018 almost all individual data sets show positive ozone trends in the upper stratosphere (1-5 hPa), with the largest recovery trend (~2.0% per decade) from B_ERA5 at ~3 hPa. Again, larger discrepancies appear in the lower stratosphere at all latitudes. In contrast to the negative trends in the NH mid-latitude region in SWOOSH and A_ERAI, B_ERA5 shows positive trends. The positive trends that also appear at SH mid-latitudes are overestimated in B_ERA5. The trends derived using simple Ordinary Least Square (OLS) method are generally in good agreement with those derived from MLR (**Figure 9**) for both SWOOSH and model simulations, confirming that they are robust. Hence, these results show that ozone trends from B_ERA5 should be considered with care.

3.3 Mean age-of-air comparison

Due to air parcels exhibiting long residence times in the stratosphere, stratospheric mean age-of-air (AoA) provides an insight into the stratospheric transport processes. In a model it is simulated simply by releasing an inert tracer from the tropical tropopause (e.g. Hall et al., 1999; Monge-Sanz et al., 2013, 2022). Simulated AoA are evaluated against

https://doi.org/10.5194/acp-2022-182
Preprint. Discussion started: 7 April 2022

observations and is considered as a standard test for stratospheric models (Waugh and Hall, 2002). Changes in AoA in the stratosphere mirror changes associated with the stratospheric mean meridional circulation (Stiller et al., 2008; Mahieu et al., 2014; Prignon et al., 2021). It should be noted that AoA captures the combined effects of the advective part of the BDC known as the residual circulation and the two-way mass exchange (mixing) on stratospheric tracer transport (Plumb, 2002; Shepherd, 2007), the effects of which might counteract each other, especially in the lowermost stratosphere (Birner and Bönisch, 2011; Garney et al., 2014; Karpechko et al., 2018). The interannual and long-term changes in the strength of the BDC are responsible for the winter-spring build-up of extratropical ozone (e.g. Fusco and Salby, 1999; Weber et al., 2003; Dhomse et al., 2006).

Ploeger et al. (2021) analysed the global stratospheric BDC using simulations of stratospheric mean AoA with the Chemical Lagrangian Model of the Stratosphere (ClaMS) driven by reanalysis (ERA5/ERA-Interim) winds and total diabatic heating rates. They found that ERA5-based results exhibit older AoA compared to results based on ERA-Interim, indicative of a significantly slower BDC for ERA5. Prignon et al. (2021) investigated the BDC variability and long-term changes using inorganic fluorine simulated by the Belgian Assimilation System for Chemical ObsErvation chemistry transport model (BASCOE CTM) driven by 5 modern reanalyses. The comparison with observations suggests an overall better representation of transport variability in ERA5 than in ERA-Interim over the period 1990-2018, especially in the NH mid-latitudes. As discussed earlier in our ozone trend analysis (Section 3.2), we find B_ERA5 shows a significant increasing trend in lower stratospheric ozone at NH mid-latitudes, while observations (SWOOSH) and A_ERAI continue to decrease after 1998. Hence, we diagnose the effect of changes in the representation of stratospheric transport by analysing variability and trends in the AoA tracer between two simulations and explore the potential causes for these inconsistencies.

https://doi.org/10.5194/acp-2022-182
Preprint. Discussion started: 7 April 2022

Atmospheric Chemistry and Physics
Open Access
EGU
Discussions

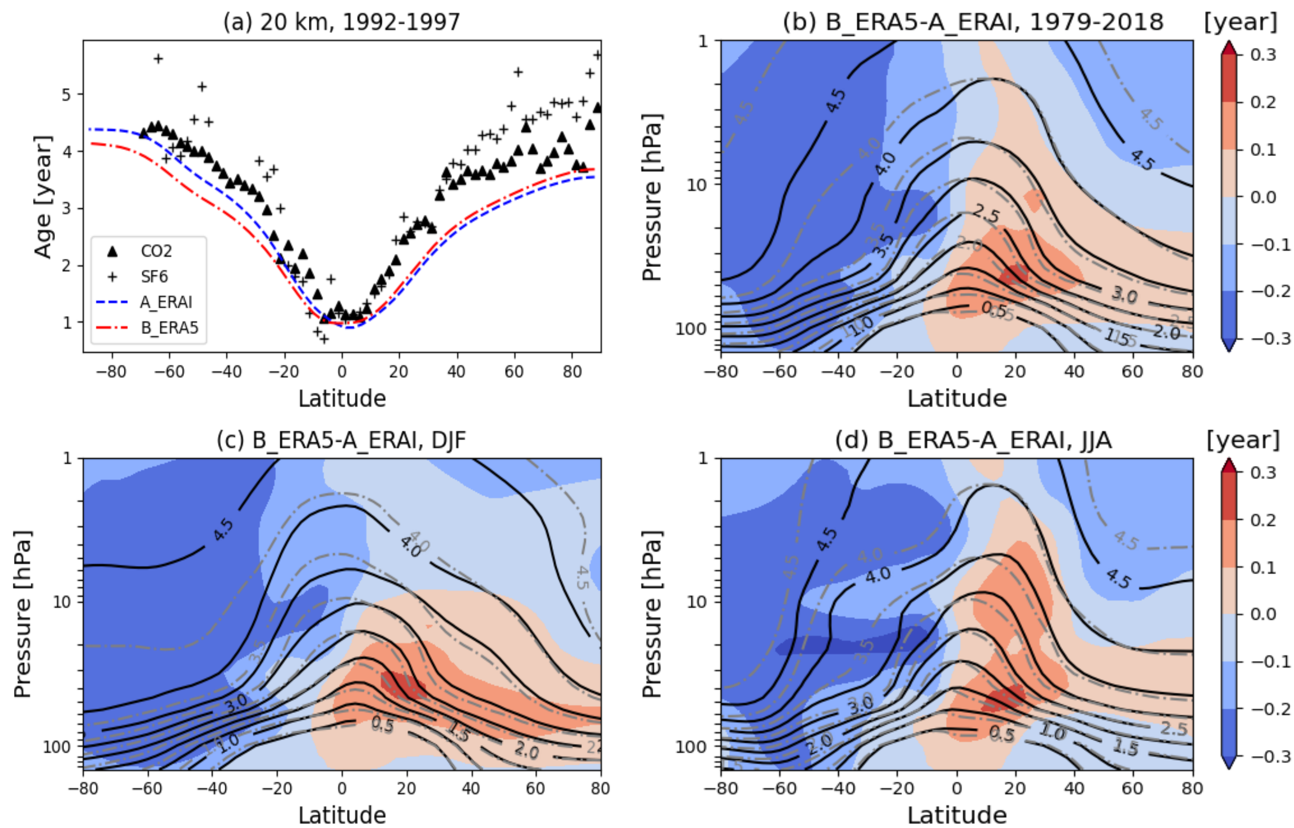

Figure 10: (a) Mean age-of-air (AoA, years) at 20 km at different latitudes from in situ observations of CO_2, SF_6 (black symbols, from Hall et al., 1999), A_ERAI (blue solid line) and B_ERA5 (red dash-dot line). (b) Pressure-latitude cross section of mean age from A_ERAI (black solid contours) and B_ERA5 (grey dash-dot contours), and their differences (B_ERA5 - A_ERAI, in red and blue shading) averaged over 1984-2018. Panels (c) and (d) are similar to (b) but for DJF and JJA means, respectively.

Figure 10a shows mean AoA at 20 km from model simulations as well as in situ CO_2 and SF_6 measurements (Hall et al., 1999). The mean AoA from A_ERAI and B_ERA5 simulations over the period 1992-1997 agree relatively well with the in situ data (better with CO_2), and both simulations show steeper gradients in AoA at SH mid-latitudes relative to NH mid-latitudes. We find that both simulations underestimate the observed mean age, especially at NH mid-latitudes. As shown in Chipperfield (2006), the use of potential temperature (θ) coordinates in the stratosphere can improve low-biased stratospheric AoA in the model using hybrid sigma-pressure (σ-p) levels. The general characteristics of the stratospheric mean age (**Figure 10b**) are evident for both A_ERAI and B_ERA5 simulations, with age increasing with both latitude and altitude (Ploeger et al., 2019, 2021). The comparison of the mean age shows that age from B_ERA5 is slightly older than that from A_ERAI in the NH stratosphere but somewhat younger in the SH stratosphere, which suggests a slower BDC in the NH but a faster BDC in the SH.

https://doi.org/10.5194/acp-2022-182
Preprint. Discussion started: 7 April 2022

Atmospheric Chemistry and Physics
Discussions

The integrated effect of BDC transport in A_ERAI and B_ERA5 is compared for mean AoA between winter and summer seasons in **Figures 10c-d**. The DJF and JJA mean comparisons are consistent with **Figure 10b**. However, in DJF (boreal wintertime) when there is a build-up in the NH, B_ERA5 shows slightly older air than A_ERAI (~0.14 year at 20 km) when compared to boreal summertime (~0.01 year at 20 km). This contrasting feature indicates some fundamental differences in the representation of BDC between two reanalysis data sets and also highlights that a slower BDC might not reduce wintertime ozone build-up at NH mid-high latitudes and B_ERA5 also shows improvements in the TCO biases in the tropics. A possible explanation is that the finer vertical resolution in ERA5 significantly alters vertical transport pathways that are critical for controlling ozone concentration as within a few kilometres in the stratosphere the ozone lifetime changes from days to a few years.

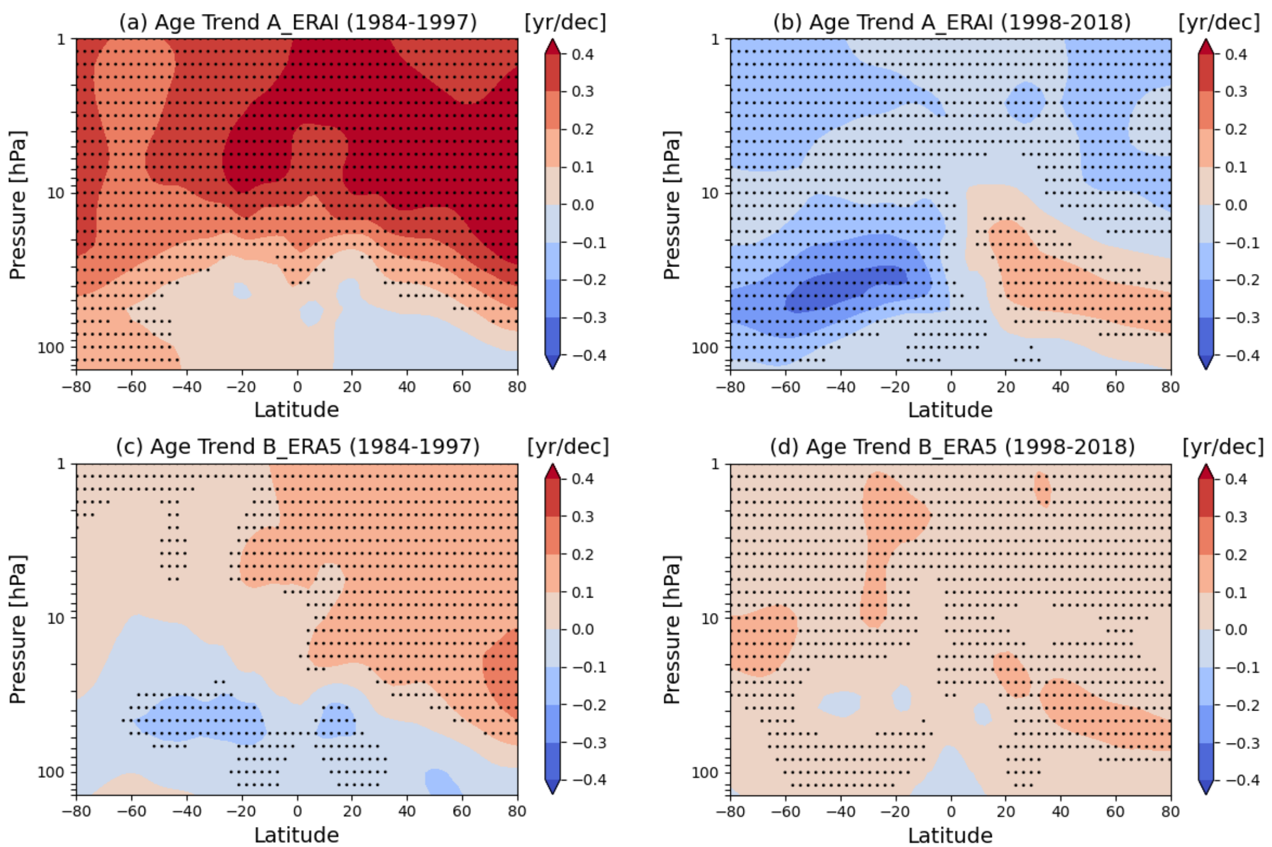

Figure 11: Mean age-of-air trends (year/decade) for the period 1984-1997 from simulations (a) A_ERAI and (c) B_ ERA5. Panels (b) and (d) are the same as (a) and (c), respectively, but for the period 1998-2018. Stippled regions indicate where the trends are statistically significant at 95% level of confidence.

AoA trends over the periods 1984-1997 and 1998-2018 from A_ERAI and B_ERA5 are shown in **Figure 11**, corresponding to the trends in ozone shown in **Figure 9**. Mean AoA trends are calculated from linear regression of the deseasonalized time series. As shown in **Figures 11a** and **c**, both A_ERAI and B_ ERA5 simulations show increasing AoA

https://doi.org/10.5194/acp-2022-182
Preprint. Discussion started: 7 April 2022

over the 1984-1997 period in the upper and middle stratosphere especially in the NH (about 0.2-0.4 year/decade). A closer look at the differences suggest weaker positive AoA trends in the upper stratosphere and larger negative trends in the lower stratosphere in B_ERA5 compared with A_ERAI. This can be confirmed by the differences of the two simulated deseasonalized AoA time series, as shown in **Figure 12**, with biases in B_ERA5 changing from positive to negative over 1984-1997.

During 1998-2018, A_ERAI shows clear positive trends in the NH and negative trends in the SH lower stratosphere (**Figure 11b**). The hemispheric dipole trend pattern in A_ERAI AoA are similar to the earlier studies (Haenel et al., 2015; Stiller et al., 2017; Ploeger et al. 2021; Monge-Sanz et al., 2022). In contrast, B_ERA5 (**Figure 11d**) shows increasing AoA trends in the whole stratosphere, indicating a decelerating BDC. The globally positive AoA trends in B_ERA5 can also be seen from **Figure 12** in which B_ERA5 shows positive biases since 2012 compared to A_ERAI. It should be noted that the positive AoA trends seen in B_ERA5 throughout the stratosphere are opposite to the negative ERA5 trends (over the 1989-2018 period) shown in Ploeger et al. (2021). They suggested the clear decrease in ERA5 mean age is not a simple linear trend and appears to be related to the increased AoA values at the beginning of the period and the step-like decreases during the 1990s. The remarkable differences in B_ERA5 mean AoA values and trend estimates (**Figures 10a** and **11d**) from the CLaMs model simulations in Ploeger et al. (2021) might be due to the different horizontal resolutions, p or θ coordinates, and/or calculation methods used. However, the differences in mid-latitude AoA trends from A_ERAI and B_ERA5 over the 1998-2018 period appear more consistent with the inorganic fluorine trends based on BASCOE CTM simulations for the 2004-2018 period (Prignon et al., 2021).

The increasing AoA in B_ERA5 after 1998 as well as the older age in the NH lower stratosphere, suggest that other transport pathways (such as downward transport/reduced transport in the troposphere) might have been responsible for the increasing ozone in the NH extratropical lower stratosphere in B_ERA5 (as shown in **Figure 9f**). In **Figure 12**, mean AoA anomalies in B_ERA5 show negative biases compared to A_ERAI from 1992 to around 2011, which is somewhat similar to the step-like changes in Ploeger et al. (2021). These changes might be associated with the representation of Mt. Pinatubo volcanic eruption induced circulation/chemistry changes (e.g. Dhomse et al., 2015; Monge-Sanz et al., 2022), transport processes as well as changes in number of observations used between these two data assimilation systems (e.g. Fujiwara et al, 2017).

https://doi.org/10.5194/acp-2022-182
Preprint. Discussion started: 7 April 2022

Atmospheric Chemistry and Physics
Discussions

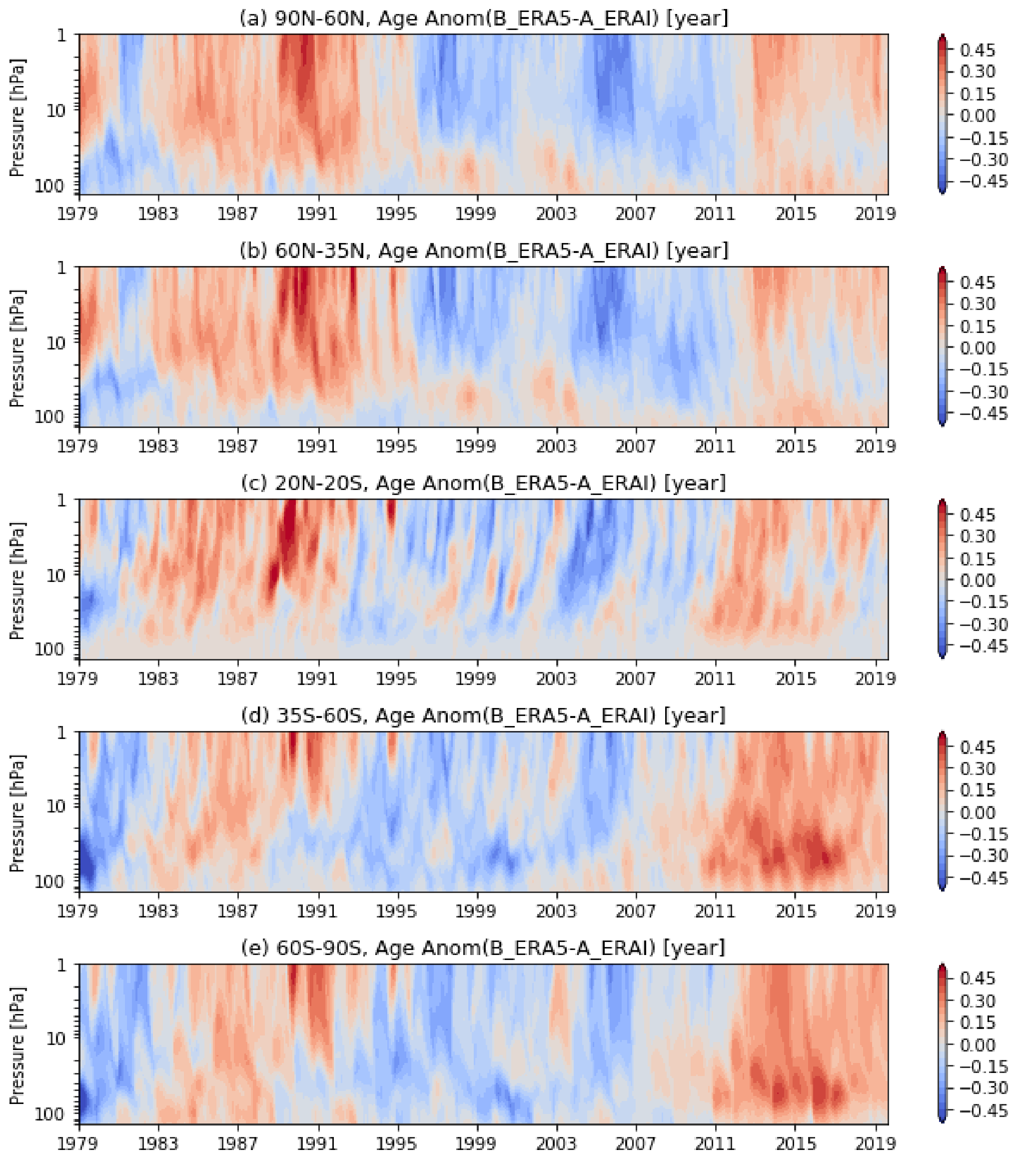

Figure 12: Pressure-time series of differences in mean age-of-air (AoA) between A_ERAI and B_ERA5 (B_ERA5 - A_ERAI) over 1979-2019 (August) for (a) 90 °N-60 °N, (b) 60 °N-35 °N, (c) 20 °N-20 °S, (d) 35 °S-60 °S and (e) 60 °S-90 °S zonal regions. Data have been deseasonalized by applying a 12-month running mean.

4 Conclusions and discussion

We have investigated the performance of two TOMCAT model simulations (A_ERAI and B_ERA5) forced with different ECMWF reanalysis datasets (ERA-Interim and ERA5). The variability and trends in total column ozone and stratospheric

https://doi.org/10.5194/acp-2022-182
Preprint. Discussion started: 7 April 2022

Atmospheric Chemistry and Physics
Discussions

ozone profiles are compared with the observation-based datasets (C3S and SWOOSH). We also analysed an AoA tracer to diagnose the impact of stratospheric transport processes on simulated ozone. Our main results are summarized as follows:

- Comparison with C3S total column ozone anomalies (1979-2019) suggests that simulation B_ERA5 shows better agreement than A_ERAI. Largest biases between the A_ERAI and B_ERA5 model simulations appear in the NH mid-high latitudes. In the tropics (20 °S-20 °N), both simulations underestimate the observed TCO, and B_ERA5 shows some improvements compared to the larger negative biases seen in A_ERAI. During winter-spring seasons in both hemispheric mid-latitudes B_ERA5 shows larger positive biases compared to A_ERAI, which suggests differences in representation of the stratospheric Brewer-Dobson circulation between these two reanalysis data sets. The PWLT-based regression model shows that compared to C3S-based trend estimates, both A_ERAI and B_ERA5 overestimate the negative trends before 1998 at both hemispheric mid-latitude bands whereas B_ERA5 overestimates the recovery since 1998.
- Compared to SWOOSH vertical ozone profiles (1984-2019), both A_ERAI and B_ERA5 underestimate the observed upper stratospheric ozone concentrations while they overestimate the middle and lower stratospheric ozone to varying degrees. B_ERA5 shows larger ozone biases in the tropics in both the upper and lower stratosphere. The larger biases between simulations A_ERAI and B_ERA5 in the lower stratosphere, where ozone concentrations are dominantly controlled by dynamical processes, largely contributes to their biases in total column ozone. The differences in upper stratospheric ozone anomalies between the two simulations are anti-correlated with the differences of temperature anomalies in the upper stratosphere, while ozone variability in the lower stratosphere is much more complicated. The PWLT-based regression model shows that both SWOOSH and A_ERAI show negative trends since 1998 in the NH extratropical lower stratosphere where, in contrast, B_ERA5 shows increasing trends.
- Analysis of the AoA tracer suggests that both A_ERAI and B_ERA5 underestimate the observation-based mean age, at NH mid-latitudes. Simulation B_ERA5 shows somewhat older AoA in the NH stratosphere but younger in the SH stratosphere compared to A_ERAI. Older air in B_ERA5 in the NH lower stratosphere, especially during boreal winter (DJF), indicates a slower BDC. However, this does not translate in reduced wintertime ozone build-up suggesting key differences between horizontal as well as vertical transport pathways between these two reanalysis data sets. During 1998-2018, A_ERAI shows a hemispheric dipole trend pattern with increasing AoA in the NH and decreasing trend in the SH lower stratosphere. In contrast, B_ERA5 shows increasing AoA in the whole stratosphere. The increasing AoA in B_ERA5 after 1998 and the older age in the NH lower stratosphere suggest other transport pathways might be responsible for the increasing ozone in the NH lower stratosphere.

Our results show that although B_ERA5 shows better agreement with observed TCO than A_ERAI, they do not confirm that B_ERA5, based on the newer reanalyses, performs better in simulating stratospheric ozone overall. The association between the simulated ozone differences and age-of-air differences suggests that simulation B_ERA5 may not yet be capable to reproduce the trend and strength of the stratospheric circulation (BDC) changes.

https://doi.org/10.5194/acp-2022-182
Preprint. Discussion started: 7 April 2022

Data availability. The satellite and climate data used in this study are available at the sources and references in the dataset section. The model data used for the figures in this paper are available on the website (https://zenodo.org, doi:10.5281/zenodo.6244759).

Author contributions. MPC and WF performed the model simulations. YL performed the data analysis and prepared the manuscript. SSD, MPC, WF, AC, YX and DG gave support for discussion, simulation and interpretation, and helped to write the paper. All authors edited and contributed to subsequent drafts of the manuscript.

Competing interests. The authors declare that they have no conflicts of interest.

Acknowledgements. We are grateful to the Copernicus Climate Change Service (C3S) for providing the global ozone dataset. The modelling work is supported by National Centre for Atmospheric Science (NCAS). We thank all providers of the climate data used in this study.

Financial Support. We acknowledge the support of the National Natural Science Foundation of China (grant no. 41675039, 91837311), the Natural Science Foundation for universities in Jiangsu province (grant no. 20KJD170001, 21KJB510007) and the Scientific Research Project of Nanjing Xiaozhuang University (grant no. 2019NXY42). This research is partially supported by the Natural Environment Research Council (grant no. NE/R001782/1), the National Centre for Earth Observation (grant no. NE/R016518/1) and NCAS (NE/R015244/1).

References

Albergel, C., Dutra, E., Munier, S., Calvet, J. C., Munoz-Sabater, J., de Rosnay, P., and Balsamo, G.: ERA-5 and ERA-Interim driven ISBA land surface model simulations: which one performs better?, Hydrol. Earth Syst. Sci., 22, 3515-3532, doi:10.5194/hess-22-3515-2018, 2018.

Ball, W. T., Alsing, J., Mortlock, D. J., Staehelin, J., Haigh, J. D., Peter, T., Tummon, F., Stübi, R., Stenke, A., Anderson, J., Bourassa, A., Davis, S. M., Degenstein, D., Frith, S., Froidevaux, L., Roth, C., Sofieva, V., Wang, R., Wild, J., Yu, P., Ziemke, J. R., and Rozanov, E. V.: Evidence for a continuous decline in lower stratospheric ozone offsetting ozone layer recovery, Atmos. Chem. Phys., 18, 1379-1394, doi:10.5194/acp-18-1379-2018, 2018.

Ball, W. T., Alsing, J., Staehelin, J., Davis, S. M., Froidevaux, L., and Peter, T.: Stratospheric ozone trends for 1985–2018: sensitivity to recent large variability, Atmos. Chem. Phys., 19, 12731-12748, doi:10.5194/acp-19-12731-2019, 2019.

Ball, W. T., Chiodo, G., Abalos, M., Alsing, J., and Stenke, A.: Inconsistencies between chemistry–climate models and observed lower stratospheric ozone trends since 1998, Atmos. Chem. Phys., 20, 9737-9752, doi:10.5194/acp-20-9737-2020, 2020.

https://doi.org/10.5194/acp-2022-182
Preprint. Discussion started: 7 April 2022

Bekki, S., Rap, A., Poulain, V., Dhomse, S., Marchand, M., Lefevre, F., Forster, P. M., Szopa, S., and Chipperfield, M. P.: Climate impact of stratospheric ozone recovery, Geophys. Res. Lett., 40, 2796-2800, doi: 10.1002/grl.50358, 2013.

Birner, T. and Bönisch, H.: Residual circulation trajectories and transit times into the extratropical lowermost stratosphere, Atmos. Chem. Phys., 11, 817–827, doi:10.5194/acp-11-817-2011, 2011.

Chehade, W., Weber, M., and Burrows, J. P.: Total ozone trends and variability during 1979-2012 from merged data sets of various satellites, Atmos. Chem. Phys., 14, 7059-7074, doi:10.5194/acp-14-7059-2014, 2014.

Chipperfield, M. P.: New version of the TOMCAT/SLIMCAT off-line chemical transport model: Intercomparison of stratospheric tracer experiments, Q. J. Roy. Meteorol. Soc., 132, 1179-1203, doi:10.1256/qj.05.51, 2006.

Chipperfield, M. P., Bekki, S., Dhomse, S., Harris, N. R., Hassler, B., Hossaini, R., Steinbrecht, W., Thiéblemont, R., and Weber, M.: Detecting recovery of the stratospheric ozone layer, Nature, 549, 211-218, 2017.

Chipperfield, M. P., Dhomse, S., Hossaini, R., Feng, W., Santee, M. L., Weber, M., Burrows, J. P., Wild, J. D., Loyola, D., and Coldewey-Egbers, M.: On the Cause of Recent Variations in Lower Stratospheric Ozone, Geophys. Res. Lett., 45, 5718-5726, doi:10.1029/2018GL078071, 2018.

Chrysanthou, A., Maycock, A. C., Chipperfield, M. P., Dhomse, S., Garny, H., Kinnison, D., Akiyoshi, H., Deushi, M., Garcia, R. R., Jöckel, P., Kirner, O., Pitari, G., Plummer, D. A., Revell, L., Rozanov, E., Stenke, A., Tanaka, T. Y., Visioni, D., and Yamashita, Y.: The effect of atmospheric nudging on the stratospheric residual circulation in chemistry–climate models, Atmos. Chem. Phys., 19, 11559–11586, doi:10.5194/acp-19-11559-2019, 2019.

Davis, S. M., Rosenlof, K. H., Hassler, B., Hurst, D. F., Read, W. G., Vömel, H., Selkirk, H., Fujiwara, M., and Damadeo, R.: The Stratospheric Water and Ozone Satellite Homogenized (SWOOSH) database: a long-term database for climate studies, Earth Syst. Sci. Data, 8, 461-490, doi:10.5194/essd-8-461-2016, 2016.

Dee, D. P., Uppala, S. M., Simmons, A. J., Berrisford, P., Poli, P., Kobayashi, S., Andrae, U., Balmaseda, M. A., Balsamo, G., Bauer, P., Bechtold, P., Beljaars, A. C. M., van de Berg, L., Bidlot, J., Bormann, N., Delsol, C., Dragani, R., Fuentes, M., Geer, A. J., Haimberger, L., Healy, S. B., Hersbach, H., Holm, E. V., Isaksen, L., Kallberg, P., Kohler, M., Matricardi, M., McNally, A. P., Monge-Sanz, B. M., Morcrette, J. J., Park, B. K., Peubey, C., de Rosnay, P., Tavolato, C., Thepaut, J. N., and Vitart, F.: The ERA-Interim reanalysis: configuration and performance of the data assimilation system, Q. J. Roy. Meteorol. Soc., 137, 553-597, doi:10.1002/qj.828, 2011.

Dhomse, S. S., Weber, M., Wohltmann, I., Rex, M., and Burrows, J. P.: On the possible causes of recent increases in northern hemispheric total ozone from a statistical analysis of satellite data from 1979 to 2003, Atmos. Chem. Phys., 6, 1165-1180, doi:10.5194/acp-6-1165-2006, 2006.

Dhomse, S. S., Chipperfield, M. P., Feng, W., and Haigh, J. D.: Solar response in tropical stratospheric ozone: a 3-D chemical transport model study using ERA reanalyses, Atmos. Chem. Phys., 11, 12773–12786, doi:10.5194/acp-11-12773-2011, 2011.

Dhomse, S. S., Chipperfield, M. P., Feng, W., Hossaini, R., Mann, G. W., and Santee, M. L.: Revisiting the hemispheric asymmetry in midlatitude ozone changes following the Mount Pinatubo eruption: A 3-D model study, Geophys. Res. Lett., 42, 3038-3047, doi:10.1002/2015gl063052, 2015.

Dhomse, S. S., Chipperfield, M., Damadeo, R., Zawodny, J., Ball, W., Feng, W., Hossaini, R., Mann, G., and Haigh, J.: On the ambiguous nature of the 11 year solar cycle signal in upper stratospheric ozone, Geophys. Res. Lett., 43, 7241–7249, doi:10.1002/2016GL069958, 2016.

Dhomse, S. S., Kinnison, D., Chipperfield, M. P., Salawitch, R. J., Cionni, I., Hegglin, M. I., Abraham, N. L., Akiyoshi, H., Archibald, A. T., Bednarz, E. M., Bekki, S., Braesicke, P., Butchart, N., Dameris, M., Deushi, M., Frith, S., Hardiman, S. C., Hassler, B., Horowitz, L. W., Hu, R. M., Jöckel, P., Josse, B., Kirner, O., Kremser, S., Langematz, U., Lewis, J., Marchand, M., Lin, M., Mancini, E., Marécal, V., Michou, M., Morgenstern, O., O'Connor, F. M., Oman, L., Pitari, G., Plummer, D. A., Pyle, J. A., Revell, L. E., Rozanov, E., Schofield, R., Stenke, A., Stone, K., Sudo, K., Tilmes, S., Visioni, D., Yamashita, Y., and Zeng, G.: Estimates of ozone return dates from Chemistry-Climate Model Initiative simulations, Atmos. Chem. Phys., 18, 8409-8438, doi:10.5194/acp-18-8409-2018, 2018.

Dhomse, S. S., Feng, W., Montzka, S. A., Hossaini, R., Keeble, J., Pyle, J. A., Daniel, J. S., and Chipperfield, M. P.: Delay in recovery of the Antarctic ozone hole from unexpected CFC-11 emissions, Nature Communications, 10, 5781, doi:10.1038/s41467-019-13717-x, 2019.

Dhomse, S. S., Arosio, C., Feng, W., Rozanov, A., Weber, M., and Chipperfield, M. P.: ML-TOMCAT: machine-learning-based satellite-corrected global stratospheric ozone profile data set from a chemical transport model, Earth Syst. Sci. Data, 13, 5711–5729, doi:10.5194/essd-13-5711-2021, 2021.

Diallo, M., Ern, M., and Ploeger, F.: The advective Brewer–Dobson circulation in the ERA5 reanalysis: climatology, variability, and trends, Atmos. Chem. Phys., 21, 7515-7544, doi:10.5194/acp-21-7515-2021, 2021.

Dietmüller, S., Garny, H., Eichinger, R., and Ball, W. T.: Analysis of recent lower-stratospheric ozone trends in chemistry climate models, Atmos. Chem. Phys., 21, 6811-6837, doi:10.5194/acp-21-6811-2021, 2021.

Douglass, A. R., Stolarski, R. S., Strahan, S. E., Oman, L. D.: Understanding differences in upper stratospheric ozone response to changes in chlorine and temperature as computed using CCMVal-2 models, J. Geophys. Res., 117(D16), 16306, 2012.

Feng, W., Chipperfield, M. P., Davies, S., von der Gathen, P., Kyro, E., Volk, C. M., Ulanovsky, A., and Belyaev, G.: Large chemical ozone loss in 2004/2005 Arctic winter/spring, Geophys. Res. Lett., 34, 10.1029/2006gl029098, 2007.

Feng, W., Chipperfield, M. P., Davies, S., Mann, G. W., Carslaw, K. S., Dhomse, S., Harvey, L., Randall, C., and Santee, M. L.: Modelling the effect of denitrification on polar ozone depletion for Arctic winter 2004/2005, Atmos. Chem. Phys., 11, 6559-6573, doi:10.5194/acp-11-6559-2011, 2011.

Feng, W., Dhomse, S. S., Arosio, C., Weber, M., Burrows, J. P., Santee, M. L., and Chipperfield, M. P.: Arctic ozone depletion in 2019/20: Roles of chemistry, dynamics and the Montreal Protocol, Geophys. Res. Lett., 48, e2020GL091911, 2021.

https://doi.org/10.5194/acp-2022-182
Preprint. Discussion started: 7 April 2022

Fioletov, V. E. and Shepherd, T. G.: Seasonal persistence of midlatitude total ozone anomalies, Geophys. Res. Lett., 30, doi: 10.1029/2002gl016739, 2003.

Fioletov, V.: Estimating the 27-day and 11-year solar cycle variations in tropical upper stratospheric ozone, J. Geophys. Res., 114, D02302, doi:10.1029/2008JD010499, 2009.

Fujiwara, M., Wright, J. S., Manney, G. L., Gray, L. J., Anstey, J., Birner, T., Davis, S., Gerber, E. P., Harvey, V. L., Hegglin, M. I., Homeyer, C. R., Knox, J. A., Krüger, K., Lambert, A., Long, C. S., Martineau, P., Molod, A., Monge-Sanz, B. M., Santee, M. L., Tegtmeier, S., Chabrillat, S., Tan, D. G. H., Jackson, D. R., Polavarapu, S., Compo, G. P., Dragani, R., Ebisuzaki, W., Harada, Y., Kobayashi, C., McCarty, W., Onogi, K., Pawson, S., Simmons, A., Wargan, K., Whitaker, J. S., and Zou, C.-Z.: Introduction to the SPARC Reanalysis Intercomparison Project (S-RIP) and overview of the reanalysis systems, Atmos. Chem. Phys., 17, 1417–1452, doi:10.5194/acp-17-1417-2017, 2017.

Fusco, A. C. and Salby, M. L.: Interannual Variations of Total Ozone and Their Relationship to Variations of Planetary Wave Activity, J. Climate, 12, 1619-1629, doi:10.1175/1520-0442(1999)012<1619:Ivotoa>2.0.Co;2, 1999.

Garny, H., Birner T., Bönisch H., and Bunzel F.: The effects of mixing on age of air, J. Geophys. Res., 119, 7015–7034, doi:10.1002/2013JD021417, 2014.

Haenel, F. J., Stiller, G. P., von Clarmann, T., Funke, B., Eckert, E., Glatthor, N., Grabowski, U., Kellmann, S., Kiefer, M., Linden, A., and Reddmann, T.: Reassessment of MIPAS age of air trends and variability, Atmos. Chem. Phys., 15, 13161-13176, doi:10.5194/acp-15-13161-2015, 2015.

Hall, T. M., Waugh, D. W., Boering, K. A., and Plumb, R. A.: Evaluation of transport in stratospheric models, J. Geophys. Res., 104, 18815-18839, doi:10.1029/1999JD900226, 1999.

Harris, N. R. P., Hassler, B., Tummon, F., Bodeker, G. E., Hubert, D., Petropavlovskikh, I., Steinbrecht, W., Anderson, J., Bhartia, P. K., Boone, C. D., Bourassa, A., Davis, S. M., Degenstein, D., Delcloo, A., Frith, S. M., Froidevaux, L., Godin-Beekmann, S., Jones, N., Kurylo, M. J., Kyrölä, E., Laine, M., Leblanc, S. T., Lambert, J. C., Liley, B., Mahieu, E., Maycock, A., de Mazière, M., Parrish, A., Querel, R., Rosenlof, K. H., Roth, C., Sioris, C., Staehelin, J., Stolarski, R. S., Stübi, R., Tamminen, J., Vigouroux, C., Walker, K. A., Wang, H. J., Wild, J., and Zawodny, J. M.: Past changes in the vertical distribution of ozone – Part 3: Analysis and interpretation of trends, Atmos. Chem. Phys., 15, 9965-9982, doi:10.5194/acp-15-9965-2015, 2015.

Hersbach, H., Bell, B., Berrisford, P., Hirahara, S., Horányi, A., Muñoz-Sabater, J., Nicolas, J., Peubey, C., Radu, R., Schepers, D., Simmons, A., Soci, C., Abdalla, S., Abellan, X., Balsamo, G., Bechtold, P., Biavati, G., Bidlot, J., Bonavita, M., De Chiara, G., Dahlgren, P., Dee, D., Diamantakis, M., Dragani, R., Flemming, J., Forbes, R., Fuentes, M., Geer, A., Haimberger, L., Healy, S., Hogan, R. J., Hólm, E., Janisková, M., Keeley, S., Laloyaux, P., Lopez, P., Lupu, C., Radnoti, G., de Rosnay, P., Rozum, I., Vamborg, F., Villaume, S., and Thépaut, J.-N.: The ERA5 global reanalysis, Q. J. Roy. Meteorol. Soc., 146, 1999-2049, doi:10.1002/qj.3803, 2020.

Hubert, D., Lambert, J. C., Verhoelst, T., Granville, J., Keppens, A., Baray, J. L., Bourassa, A. E., Cortesi, U., Degenstein, D. A., Froidevaux, L., Godin-Beekmann, S., Hoppel, K. W., Johnson, B. J., Kyrölä, E., Leblanc, T., Lichtenberg, G., Marchand,

https://doi.org/10.5194/acp-2022-182
Preprint. Discussion started: 7 April 2022

M., McElroy, C. T., Murtagh, D., Nakane, H., Portafaix, T., Querel, R., Russell Iii, J. M., Salvador, J., Smit, H. G. J., Stebel, K., Steinbrecht, W., Strawbridge, K. B., Stübi, R., Swart, D. P. J., Taha, G., Tarasick, D. W., Thompson, A. M., Urban, J., van Gijsel, J. A. E., Van Malderen, R., von der Gathen, P., Walker, K. A., Wolfram, E., and Zawodny, J. M.: Ground-based assessment of the bias and long-term stability of 14 limb and occultation ozone profile data records, Atmos. Meas. Tech., 9, 2497-2534, doi:10.5194/amt-9-2497-2016, 2016.

Karpechko, A. Yu., Maycock, A. C., Abalos, M., Akiyoshi, H., Arblaster, J. M., Garfinkel, C. I., Rosenlof, K. H., Sigmond, M.: Stratospheric ozone changes and climate, Chapter 5 of scientific assessment of ozone depletion: 2018, global ozone research and monitoring project, Report No.58, World Meteorological Organization, Geneva, Switzerland, 2018.

Li, Y., Chipperfield, M. P., Feng, W., Dhomse, S. S., Pope, R. J., Li, F., and Guo, D.: Analysis and attribution of total column ozone changes over the Tibetan Plateau during 1979–2017, Atmos. Chem. Phys., 20, 8627-8639, doi: 10.5194/acp-20-8627-2020, 2020.

Mahieu, E., Chipperfield, M. P., Notholt, J., Reddmann, T., Anderson, J., Bernath, P. F., Blumenstock, T., Coffey, M. T., Dhomse, S. S., Feng, W., Franco, B.: Recent Northern Hemisphere stratospheric HCl increase due to atmospheric circulation changes, Nature, 515, 104-107, doi: 10.1038/nature13857, 2014.

Marsh, D. R., Lamarque, J.-F., Conley, A. J., and Polvani, L. M.: Stratospheric ozone chemistry feedbacks are not critical for the determination of climate sensitivity in CESM1 (WACCM), Geophys. Res. Lett., 43, 3928-3934, doi:10.1002/2016GL068344, 2016.

Monge-Sanz, B. M., Chipperfield, M. P., Dee, D. P., Simmons, A. J., and Uppala, S. M.: Improvements in the stratospheric transport achieved by a chemistry transport model with ECMWF (re)analyses: identifying effects and remaining challenges, Q. J. Roy. Meteorol. Soc., 139, 654-673, doi: 10.1002/qj.1996, 2013.

Monge-Sanz, B. M., Birner, T., Chabrillat, S., Diallo, M., Haenel, F., Konopka, P., Legras, B., Ploeger, F., Reddmann, T., Stiller, G., Wright, J. S., Abalos, M., Boenisch, H., Davis, S., Garny, H., Hitchcock, P., Miyazaki, K., Roscoe, H. K., Sato, K., Tao, M., Waugh, D.: Brewer-Dobson Circulation, Chapter 5 of SPARC Reanalysis Intercomparison Project (S-RIP) Final Report, SPARC Report No. 10, 2022.

McLandress, C., Plummer, D. A., and Shepherd, T. G.: Technical Note: A simple procedure for removing temporal discontinuities in ERA-Interim upper stratospheric temperatures for use in nudged chemistry-climate model simulations, Atmos. Chem. Phys., 14, 1547–1555, doi:10.5194/acp-14-1547-2014, 2014.

Orbe, C., Wargan, K., Pawson, S., and Oman, L. D.: Mechanisms Linked to Recent Ozone Decreases in the Northern Hemisphere Lower Stratosphere, J. Geophys. Res.-Atmospheres, 125, e2019JD031631, doi:10.1029/2019JD031631, 2020a.

Orbe, C., Plummer, D. A., Waugh, D. W., Yang, H., Jöckel, P., Kinnison, D. E., Josse, B., Marecal, V., Deushi, M., Abraham, N. L., Archibald, A. T., Chipperfield, M. P., Dhomse, S., Feng, W., and Bekki, S.: Description and Evaluation of the specified-dynamics experiment in the Chemistry-Climate Model Initiative , Atmos. Chem. Phys., 20, 3809–3840, doi:10.5194/acp-20-3809-2020, 2020b.

Ploeger, F., Abalos, M., Birner, T., Konopka, P., Legras, B., Müller, R., and Riese, M.: Quantifying the effects of mixing and residual circulation on trends of stratospheric mean age of air, Geophys. Res. Lett., 42, 2047-2054, doi:10.1002/2014GL062927, 2015.

Ploeger, F., Legras, B., Charlesworth, E., Yan, X., Diallo, M., Konopka, P., Birner, T., Tao, M., Engel, A., and Riese, M.: How robust are stratospheric age of air trends from different reanalyses?, Atmos. Chem. Phys., 19, 6085–6105, doi:10.5194/acp-19-6085-2019, 2019.

Ploeger, F., Diallo, M., Charlesworth, E., Konopka, P., Legras, B., Laube, J. C., Grooß, J. U., Günther, G., Engel, A., and Riese, M.: The stratospheric Brewer–Dobson circulation inferred from age of air in the ERA5 reanalysis, Atmos. Chem. Phys., 21, 8393-8412, doi: 10.5194/acp-21-8393-2021, 2021.

Plumb, R.: Stratospheric transport, J. Meteorol. Soc. Jpn., 80, 793– 809, doi:10.2151/jmsj.80.793, 2002.

Prignon, M., Chabrillat, S., Friedrich, M., Smale, D., Strahan, S. E., Bernath, P. F., Chipperfield, M. P., Dhomse, S. S., Feng, W., Minganti, D., Servais, C., Mahieu, E.: Stratospheric fluorine as a tracer of circulation changes: Comparison between infrared remote-sensing observations and simulations with five modern reanalyses, J. Geophys. Res., 126, e2021JD034995, doi:10.1029/2021JD034995, 2021.

Randel, W. J. and Cobb, J. B.: Coherent variations of monthly mean column ozone and lower stratospheric temperature, J. Geophys. Res., 99, 5433–5447, doi: 10.1029/93JD03454, 1994.

Randel, W. J. and Wu, F.: A stratospheric ozone profile data set for 1979–2005: Variability, trends, and comparisons with column ozone data, J. Geophys. Res., 112, D06313, doi:10.1029/2006JD007339, 2007.

Reinsel, G. C., Weatherhead, E. C., Tiao, G. C., Miller, A. J., Nagatani, R. M., Wuebbles, D. J., and Flynn, L. E.: On detection of turnaround and recovery in trend for ozone, J. Geophys. Res., 107, doi:10.1029/2001jd000500, 2002.

Schoeberl, M. R., Douglass, A. R., Zhu, Z., and Pawson, S.: A comparison of the lower stratospheric age spectra derived from a general circulation model and two data assimilation systems, J. Geophys. Res., 108, doi:10.1029/2002JD002652, 2003.

Shepherd, T. G.: Transport in the middle atmosphere, J. Meteorol. Soc. Jpn., 85, 165–191, doi: 10.2151/jmsj.85B.165, 2007.

Simmons, A, Soci, C, Nicolas, J, Bell, B, Berrisford, P, Dragani, R, Flemming, J, Haimberger, L, Healy, S, Hersbach, H, Horányi, A, Inness, A, Munoz-Sabater, J, Radu, R, Schepers, D.: Global stratospheric temperature bias and other stratospheric aspects of ERA5 and ERA5.1, ECMWF Technical Memoranda, 859, doi: 10.21957/rcxqfmg0, 2020.

Sofieva, V. F., Kyrola, E., Laine, M., Tamminen, J., Degenstein, D., Bourassa, A., Roth, C., Zawada, D., Weber, M., Rozanov, A., Rahpoe, N., Stiller, G., Laeng, A., von Clarmann, T., Walker, K. A., Sheese, P., Hubert, D., van Roozendael, M., Zehner, C., Damadeo, R., Zawodny, J., Kramarova, N., and Bhartia, P. K.: Merged SAGE II, Ozone_cci and OMPS ozone profile dataset and evaluation of ozone trends in the stratosphere, Atmos. Chem. Phys., 17, 12533-12552, doi:10.5194/acp-17-12533-2017, 2017.

Solomon, S., Portman, R. W., Garcia, R. R., Thomason, L. W., Poole, L. R., and McCormack, M. P.: The role of aerosol variations in anthropogenic ozone depletion at northern midlatitudes, J. Geophys. Res., 101, 6713–6727, doi: 10.1029/95JD03353, 1996.

Solomon, S., Ivy, D. J., Kinnison, D., Mills, M. J., Neely, R. R., and Schmidt, A.: Emergence of healing in the Antarctic ozone layer, Science, 353, 269-274, doi:10.1126/science.aae0061, 2016.

SPARC: SPARC/IO3C/GAW Report on Long-term Ozone Trends and Uncertainties in the Stratosphere, SPARC Report No. 9, doi: 10.17874/f899e57a20b, 2019.

Steinbrecht, W., Froidevaux, L., Fuller, R., Wang, R., Anderson, J., Roth, C., Bourassa, A., Degenstein, D., Damadeo, R., Zawodny, J., Frith, S., McPeters, R., Bhartia, P., Wild, J., Long, C., Davis, S., Rosenlof, K., Sofieva, V., Walker, K., Rahpoe, N., Rozanov, A., Weber, M., Laeng, A., von Clarmann, T., Stiller, G., Kramarova, N., Godin-Beekmann, S., Leblanc, T., Querel, R., Swart, D., Boyd, I., Hocke, K., Kampfer, N., Barras, E. M., Moreira, L., Nedoluha, G., Vigouroux, C., Blumenstock, T., Schneider, M., Garcia, O., Jones, N., Mahieu, E., Smale, D., Kotkamp, M., Robinson, J., Petropavlovskikh, I., Harris, N., Hassler, B., Hubert, D., and Tummon, F.: An update on ozone profile trends for the period 2000 to 2016, Atmos. Chem. Phys., 17, 10675-10690, doi:10.5194/acp-17-10675-2017, 2017.

Stiller, G. P., von Clarmann, T., Höpfner, M., Glatthor, N., Grabowski, U., Kellmann, S., Kleinert, A., Linden, A., Milz, M., Reddmann, T., Steck, T., Fischer, H., Funke, B., López-Puertas, M., and Engel, A.: Global distribution of mean age of stratospheric air from MIPAS SF6 measurements, Atmos. Chem. Phys., 8, 677-695, doi:10.5194/acp-8-677-2008, 2008.

Stiller, G., Laeng, A., von Clarmann, T., Walker, K. A., Sheese, P., Hubert, D., van Roozendael, M., Zehner, C., Damadeo, R., Zawodny, J., Kramarova, N., and Bhartia, P. K.: Merged SAGE II, Ozone_cci and OMPS ozone profile dataset and evaluation of ozone trends in the stratosphere, Atmos. Chem. Phys., 17, 12533-12552, doi:10.5194/acp-17-12533-2017, 2017.

Stone, K. A., Solomon, S., and Kinnison, D. E.: On the Identification of Ozone Recovery, Geophys. Res. Lett., 45, 5158-5165, doi:10.1029/2018GL077955, 2018.

Tegtmeier, S., Fioletov, V. E. and Shepherd, T. G.: Seasonal persistence of northern low- and middle-latitude anomalies of ozone and other trace gases in the upper stratosphere, J. Geophys. Res., 113, D21308, doi:10.1029/2008JD009860, 2008.

Wargan, K., Orbe, C., Pawson, S., Ziemke, J. R., Oman, L. D., Olsen, M. A., Coy, L., and Emma Knowland, K.: Recent Decline in Extratropical Lower Stratospheric Ozone Attributed to Circulation Changes, Geophys. Res. Lett., 45, 5166-5176, doi:10.1029/2018GL077406, 2018.

Waugh, D. and Hall, T.: Age of stratospheric air: Theory, observations, and models, Rev. Geophys., 40, 1-1-1-26, doi:10.1029/2000RG000101, 2002.

Weber, M., Dhomse, S., Wittrock, F., Richter, A., Sinnhuber, B.-M., and Burrows, J. P.: Dynamical control of NH and SH winter/spring total ozone from GOME observations in 1995–2002, Geophys. Res. Lett., 30, doi:10.1029/2002GL016799, 2003.

https://doi.org/10.5194/acp-2022-182
Preprint. Discussion started: 7 April 2022

Weber, M., Coldewey-Egbers, M., Fioletov, V. E., Frith, S. M., Wild, J. D., Burrows, J. P., Long, C. S., and Loyola, D.: Total ozone trends from 1979 to 2016 derived from five merged observational datasets - the emergence into ozone recovery, Atmos. Chem. Phys., 18, 2097-2117, doi:10.5194/acp-18-2097-2018, 2018.

WMO: Scientific Assessment of Ozone Depletion: 2014 Global Ozone Research and Monitoring Project Report, World Meteorological Organization, p. 416, Geneva, Switzerland, 2014.

WMO: Scientific Assessment of Ozone Depletion: 2018, Global Ozone Research and Monitoring Project Report, World Meteorological Organization, p. 588, Geneva, Switzerland, 2018.